GAS SEPARATION MEMBRANES MADE THROUGH THERMAL REARRAGEMENT OF *ORTHO*-METHOXYPOLYIMIDES. INFLUENCE OF THE ORTHO SUBSTITUTION ON THE FINAL PROPERTIES

(empty line 6 pt)

Bibiana Comesaña-Gándara[1,2,3,4], José G. de la Campa[1], Antonio Hernández[2], Young Moo Lee[4], Angel E. Lozano[1,2,3,*], Javier de Abajo[1,*]

(empty line 6 pt)

[1]Institute of Polymer Science and Technology, ICTP-CSIC, Madrid, Spain

[2]SMAP UA-UVA_CSIC, University of Valladolid, Valladolid, Spain

[3]IU Cinquima, University of Valladolid, Valladolid, Spain

[4]Department of Energy Engineering, Hanyang University, Seoul 133-791, Republic of Korea

Summary

Ortho-methoxypolyimides were prepared by the classical chemical imidization method and also by azeotropic imidization, using 3,3'-dimethoxybenzidine (DMAB) and hexafluoroisopropylidene diphthalic anhydride (6FDA) as monomers. High molecular weights were achieved by both methods, and the physical properties of the materials were investigated by spectroscopic and thermal analytical techniques. Polymers exhibited excellent thermal properties and film-forming ability, which allowed them to be tested as dense membranes for gas separation after a convenient treatment at high temperature (450 °C) to promote thermal rearrangement (TR). Spectroscopic evidences

indicated that the final composition of the TR materials seemed not to correspond to TR-polibenzoxazoles, as it is the case when *ortho*-hydroxypolyimides are exposed to similar thermal treatments. A detailed study was carried out with the purpose of elucidating the actual mechanism of rearrangement, comparing *ortho*-hydroxypolyimides and *ortho*-acetylpolyimides with the *ortho*-methoxypolyimides obtained in this work. Results led to the conclusion that the chemical nature of the final TR materials attained from *ortho*-methoxypolyimides is rather complex because imide, cyclolactam and benzoxazole groups seems to be formed under thermal treatment, and the proportion of the different moieties greatly depends on the *ortho*-substituent, on the synthesis route used to prepare the polyimide and on the time-temperature schedule applied in the thermal rearrangement. The gas permeation properties exhibited by thermally treated *ortho*-methoxypolyimides compared very well with those of other TR-PBOs reported so far, showing O_2 permeability of 94 barrers and CO_2 permeability of 540 Barrers.

1. Introduction

Polymer membranes have been widely recognized as high value-added materials, in concurrence with classical separation techniques, for the separation of gases, because membranes offer a more energy-efficient separation process than other techniques [1–5]. In addition, membrane technology is a much more environmentally friendly process with low footprint than, for instance, traditional absorptive technologies. In this regard, some application examples of industrial interest can be mentioned: O_2 or N_2 enrichment [6,7], natural gas sweetening [8,9], air drying [10,11], recovering of H_2 from the purges of ammonia synthesis or syngas production [12,13], recovering of toxic, volatile monomers as vinyl chloride [14], olefin/paraffin separation [15–17], recovering of CO_2

and acid gases from flue gas mixtures [18,19], etc.

For a polymer membrane to be a potential candidate for gas separation, it must show excellent separation properties, which means that it must offer high permeability (gas flux) and high selectivity (separation ability) at the same time. Gas transport through polymers membranes proceeds by a sorption-diffusion mechanism that involves both diffusion of gas molecules through the polymer material and interactions of the gas and the polymer at molecular scale. These processes can be defined in terms of the diffusivity coefficient (kinetic component) and the solubility coefficient (thermodynamic component), as depicted in Eq. 1:

$$P = D \cdot S \qquad (1)$$

The existence of a trade-off between permeability and selectivity has been clearly observed [20,21]. Due to this circumstance, most polymers show a balanced behavior, in such a way that a high permeability means a poor selectivity and *vice versa*. It explains the great efforts devoted to find out polymer compositions that assure at the same time good permeability and selectivity [22]. Several authors have proposed diverse ways of circumventing that trade-off in order to discover new gas separation materials with enhanced properties [citas].

In this context, a new class of polymeric materials has recently been developed, which offers a suitable approach for making efficient gas separation membranes. Aromatic polyimides (PIs) containing free –OH groups *ortho*-positioned respect to the imide ring have achieved great importance as they can be converted into polybenzoxazoles (TR-PBOs) by a controlled thermal rearrangement in solid state at high temperatures. Although some controversy still exists about the mechanism

responsible of this thermal rearrangement, the experimental evidence states that the final polybenzoxazole materials are particularly suitable for gas separation operations. In the pioneering work of Park et al. [23] permeabilities for CO_2 well over 1000 Barrers were reported for the thermally treated *ortho*-hydroxypolyimide derived from 2,2′-bis (3-amino-4-hydroxyphenyl)-hexafluoropropane (APAF) and hexafluoroisopropylidene diphthalic anhydride (6FDA). These outstanding results have pushed the membrane community to make additional efforts to optimize the methods and to seek alternative monomers, to improve the whole process of synthesis and to find out an attractive combination of economics, process feasibility and gas separation performance []. Fluorinated monomers are expensive, and even very expensive, and therefore other aromatic monomers, particularly wholly aromatic diamines derived from the biphenylene residue, have been assayed, and promising results have been achieved until now []. On the other side, to assure an easy processing of the *ortho*-hydroxypolyimides the use of dianhydride 6FDA seems to be necessary to rely on soluble polyimides, which can eventually be transformed into membranes by casting of polymer solutions.

The generally accepted mechanism for the imide-to-polybenzoxazole thermal rearrangement involves the decarboxylation of the *ortho*-hydroxypolyimide at very high temperature (well over 350 °C) through the previous formation of a carboxy-benzoxazole, with further elimination of a CO_2 molecule [24]. Additionally, other functionalized polyimides have been studied as precursors, particularly polyimides containing *ortho*-ester groups [25]. The use of esters instead of hydroxyl free groups seems to eventually render PBOs that show slightly higher permeation performance than those prepared from *ortho*-hydroxy polyimides, and in addition *ortho*-ester polyimides offer simultaneously a somewhat better solubility and a lower glass transition temperature. Guo et al. have recently reported a conscientious study about the

effects of different *ortho*-functional groups on the transformation of polyimide precursor into polybenzoxazoles and on the permeation properties [25]. These authors observed that using *ortho*-ester polyimides significantly affected the rearrangement process, and that changing –OH groups by RCOO- groups helps for a gain in permeability thanks to the increment of free volume in the precursor, provided by the voluminous ester group compared to the hydroxyl group.

Based on these antecedents, and looking for new routes to TR-PBO polymers, a study has been performed on the preparation and evaluation of TR-PBO materials obtained from *ortho*-methoxy-containing polyimides. The thermal rearrangement of *ortho*-methoxy-polyimides to TR-PBOs was very early reported [26], but a conscientious study of the process was not done at that time, nor any investigation on gas permeation properties was performed. Additionally, polybenzoxazoles have been attained from *ortho*-methoxy aromatic polyamides in some instances, mainly looking for a substantial thermal resistance increment of the precursor polyamides [27]. Other authors have followed this approach to prepare PBOs with various purposes [28,29]. However, these precursors with side methoxy groups have not been studied for TR-PBO materials that could be tested for gas separation applications.

In this work, we are reporting the preparation of soluble *ortho*-methoxy polyimides made from 6FDA dianhydride and 3,3′-dimethoxybenzidine, which is a comparatively low-priced monomer. The conversion of this precursor into TR-PBO at high temperature has been the object of a careful study, focusing our interest on the effect of the time-temperature schedule on the final properties of films fabricated from the precursor. Special attention has been given to the possible reactions occurring along the thermal treatment, in comparison with *ortho*-hydroxy and *ortho*-acetylpolyimides of similar structure and to the permeation properties of the final films in comparison with

earlier reported TR-PBOs.

2. Experimental

2.1. Materials

Chlorotrimethylsilane (CTMS), pyridine (Py), 4-dimethylaminopyridine (DMAP), *o*-xylene, acetic anhydride and anhydrous *N*-methyl-2-pyrrolidinone (NMP) were all provided by Aldrich (Milwaukee, USA) and used as received. Aromatic diamines 3,3´-dihydroxybenzidine (HAB) and 3,3´-dimethoxybenzidine (DMAB) were supplied by TCI Europe (Amsterdam, Holland) and Aldrich (Milwaukee, USA), respectively. HAB was dried at 120 ºC for 5 h under vacuum and DMAB was sublimed prior to be used. 2,2´-bis(3,4-dicarboxyphenyl)hexafluoropropane dianhydride (6FDA) was purchased from Cymit Química (Barcelona, Spain) and sublimed just before use.

2.2. Synthesis of precursor polyimides

2.2.1. Polyimides derived from 6FDA and HAB: Polyimide with free ortho-hydroxyl groups via azeotropic imidization (PI-OH) and polyimide with ortho-acetyl groups via chemical imidization (PI-OAc)

The formation of the hydroxyl-containing poly(amic acid) intermediates (*HPAA*) is common for both synthesis, with the exception of the solvent employed in the reaction. For the chemical cycloimidization process, DMAc was used as a solvent, while NMP was chosen in the case of azeotropic imidization to facilitate the water removal. *HPAA* intermediates were prepared by the following general route: 10.0 mmol of HAB diamine and 10 mL of the chosen solvent were added to a round bottomed three-necked flask and stirred at room temperature under dry nitrogen atmosphere. When the solid was entirely dissolved, the solution was cooled to 0 °C and the required

amount of CTMS (1 mol/mol reactive group) was added to the solution, followed by Py (1 mol/mol reactive group) and DMAP (0.1 mol/mol Py). The temperature was subsequently raised to room temperature and maintained for 15 min to ensure the formation of the silylated diamine. After this time, the solution was cooled to 0 °C once again, and a stoichiometric amount of 6FDA (10.0 mmol) was carefully added followed by 10 mL of solvent to rinse the inner flask walls. The reaction mixture was stirred for 15 min and then the temperature was raised up to room temperature and left overnight to form the *HPAA* intermediate.

To attain the final polyimide with -OH groups in *ortho*-position, polyimide designated as *PI-OH*, *o*-xylene (20 mL) as an azeotropic agent was added to the *HPAA* solution, which was vigorously stirred and heated for 6 h at 180 °C to promote cycloimidization. During this step, the water released from the ring-closure reaction was separated as a xylene azeotrope, along with silanol and other siloxane by-products derived from the use of the silylating agent. Additional *o*-xylene was stripped out from the polymer solution, which was then cooled to room temperature and precipitated in distilled water. The polymer thus obtained was washed several times with water, with a mixture of water/ethanol (1/1) and with ethanol, and finally dried in a convection oven at 150 ºC for 12 h under vacuum. ***PI-OH***: η_{inh} (dL/g) = 1.51. ^{1}H-NMR (DMSO-d_6, 500 MHz): 10.23 (s, 2H, OH), 8.27 (d, 2H), 8.08 (d, 2H), 7.87 (s, 2H), 7.46 (d, 2H), 7.29 (s, 2H), 7.27 (s, 2H). FT-IR (film): ν(-OH) at 3401 cm^{-1}, imide ν(C=O) at 1785 and 1715 cm^{-1}, imide ν(C-N) at 1378 cm^{-1}, imide ν(C-N-C) at 1099 cm^{-1}.

In order to obtain -OAc groups in the final polyimide structure, polyimide coded as *PI-OAc*, the *HPAA* intermediate was chemically imidized adding to the solution a mixture of acetic anhydride (80 mmol, 4 mol/mol reactive group) and Py (80 mmol, 4 mol/mol reactive group). The solution was stirred for 6 h at room temperature and 1 h

further at 60 ºC to promote whole imidization. The viscous polyimide solution was cooled at room temperature and poured onto water and the precipitate formed was repeatedly washed with water and with a mixture of water/ethanol (1/1), and finally dried in a vacuum oven at 150 ºC overnight. ***PI-OAc***: η_{inh} (dL/g) = 0.62. ^{1}H-NMR (DMSO-d_6, 500 MHz): 8.22 (d, 2H), 8.00 (d, 2H), 7.86 (s, 2H), 7.80 (m, 2H), 7.68 (d, 2H), 2.16 (s, 6H, CH_3). FT-IR (film): imide ν(C=O) at 1778 and 1724 cm^{-1}, imide ν(C-N) at 1370 cm^{-1}, imide ν(C-N-C) at 1096 cm^{-1}.

2.2.2. Polyimides derived from 6FDA and DMAB via chemical imidization (PI-OMe)

A three-necked flask was charged with 10 mmol of diamine DMAB and 10 mL of DMAc as solvent. The mixture was cooled to 0 ºC and the needed amount of CTMS (20 mmol) was incorporated, followed by Py (20 mmol) and DMAP (2 mmol). The solution was let warm to room temperature and was stirred for 15 min to ensure the formation of the silylated diamine. After this time, the solution was cooled to 0 °C again and 6FDA (10.0 mmol) was added followed by 10 mL of DMAc. After 15 minutes stirring at 0 ºC, temperature was raised up to room temperature and left overnight to form the methoxy-containing poly(amic acid) intermediate designated as *MeOPAA*. Subsequently, the *MeOPAA* intermediate was cyclized to the corresponding polyimide via chemical imidization adding to the solution a mixture of acetic anhydride (80 mmol, 4 mol/mol reactive group) and Py (80 mmol, 4 mol/mol reactive group). In order to promote the complete imidization the solution was stirred for 6 h at room temperature and 1 h further at 60 ºC. The polyimide solution was cooled at room temperature and poured onto water. The precipitate obtained was thoroughly washed with water and with ethanol, and dried at 150 ºC for 12 h under vacuum. ***PI-OMe***: η_{inh} (dL/g) = 0.59. ^{1}H-NMR (DMSO-d_6, 500 MHz): 8.19 (d, 2H), 8.00 (d, 2H), 7.86 (s, 2H), 7.53 (s, 2H), 7.52

(d, 2H), 7.46 (d, 2H), 3.88 (s, 6H, CH_3), FT-IR (film): imide ν(C=O) at 1787 and 1724 cm^{-1}, imide ν(C-N) at 1373 cm^{-1}, imide ν(C-N-C) at 1099 cm^{-1}.

2.3. Formation of polyimide films and subsequent thermal treatment.

To prepare polyimide films, 10 wt % polyimide solutions in NMP or DMAc (the same solvent used for each polyimide synthesis was selected) were filtered through a 3.1 μm glass-fiber syringe filter and cast onto well-leveled glass plates. The films were dried at 60 ºC overnight to remove the most of the solvent and then placed in a vacuum oven. The polyimide film was progressively heated to 250 ºC, holding for 1 h at 100 ºC, 150 ºC, 200 ºC and 250 ºC under vacuum to remove the residual solvent. Self-supported films were stripped off the glass plate, washed with distilled water, and dried at 130 ºC, under vacuum, overnight. Film thicknesses were between 40 and 50 μm and, in all cases, suitable film uniformity was verified by measuring the film thickness standard deviation, which was lower than 5 %. All polyimide samples were cut into 3 cm x 3 cm defect-free pieces and placed between ceramic plates, to avoid film rolling at elevated temperatures, in a muffle furnace under an inert gas. In order to completely remove solvent and to ensure full imide ring closure, all polyimide films were heated at a rate of 5 ºC/min to 300 ºC and held for 2h in the case of *PI-OH* film and 1h for *PI-OAc* and *PI-OMe* films, under a nitrogen flow of 0.3 L/min.

The precursor polyimide membranes were converted into TR membranes by a further thermal treatment. Thus, the polyimide membranes were heated to 350 ºC, 400 ºC and 450 ºC at a rate of 5 ºC min^{-1}, and maintained for the desired amount of time (30 min or 1 h) in a high-purity nitrogen atmosphere, following the protocol described in literature [30], in such way that the samples were exposed to thermal treatments similar to other previously reported. The cooling protocol consisted on allowing the furnace to

reach room temperature at a rate not greater than 10 ºC min^{-1}. The thermally treated membranes, obtained from the *PI-OH*, *PI-OAc* and *PI-OMe* precursor polyimides, were designated as TR-OHX, TR-OAcX and TR-OMeX, respectively, where X indicates the value of final temperature applied to the samples.

2.4. Polyimide and membrane characterizations.

Structural differences between polyimides were confirmed by ^{1}H-NMR spectra obtained from a Varian System 500 nuclear magnetic resonance (NMR) spectrometer operating at 500 MHz.

A Perkin Elmer Fourier transform infrared spectrometer (FT-IR) with Universal ATR Sampling Accessory was used to characterize the precursor polyimides and TR-PBO films. In addition, FT-IR was used to prove the conversion of the precursor polyimide films into PBOs. The scan range was from 4000 to 650 cm^{-1}.

Inherent viscosities of polyimide precursors were evaluated at 30 ºC with an automated Canon-Ubbelohde suspended level viscometer using NMP as solvent. The polymer concentration was 0.5 g/dL in every case.

Glass transition temperatures (T_g) of polyimide films were determined by modulated temperature differential scanning calorimetry (MDSC) analyses on a TA Q-2000 calorimeter (TA Instruments, DE, USA). MDSC allows separation of the *reversing* contribution to the average heat flow (attributed to the heat capacity), as well as the *non-reversing* contribution to the average heat flow (attributed to the kinetic effects such as enthalpy recovery or recrystallization. The temperature calibration was performed by taking the onset of the endothermic melting peak of several calibration standards: octane (T_m = 217.26 K), indium (T_m = 430.61 K) and zinc (T_m = 693.38 K). The organic standard was a high-purity Fluka product, while the metal standards were

supplied by TA Instruments Inc. Enthalpy was calibrated using indium (melting enthalpy $\Delta_m H$ = 28.71 J g^{-1}). The module of the complex heat capacity was calibrated by measuring with sapphire in the studied temperature range and for the frequencies of modulation used in the experiments. An underlying heating ramp of 5 °C min^{-1} to 450 ºC was accomplished with a modulation period of 40 s and with amplitude of the temperature modulation of 1.5 °C. T_gs were attained from the *reversing* heat flow signal.

Thermogravimetric analyses (TGA) were conducted on a TA Q-500 thermobalance (TA Instruments, DE, USA), combined with a mass spectrometer (MS) ThermoStar^{TM} GSD 301T (Pfeiffer Vacuum GmbH, Germany). Dynamic ramp scans were run at 10 ºC min^{-1} to find out about thermal stability characteristics as well as the thermal rearrangement, in the temperature range from 60 to 850 ºC. Furthermore, isothermal thermogravimetric analyses were carried out in order to adjust the most appropriate thermal treatment settings for TR films preparation and to estimate the percent conversion from the polyimide precursors to the final TR-PBOs. Therefore, polyimide film samples, thermally treated at 300 ºC, were heated to the selected rearrangement temperature (350 ºC, 400 ºC and 450 ºC) at a heating rate of 5 ºC min^{-1}, and held isothermally for 3 h. The purge gas was nitrogen (60 mL min^{-1}) and the sample mass was around 5 mg.

Intermolecular distances of PI precursor membranes and TR-PBO membranes were determined by wide angle X-ray scattering (WAXS) experiments, which were performed in the reflection mode at room temperature by using a Bruker D8 Advance system fitted with a Goebel mirror and provided with a PSD Vantec detector. Cu-$K\alpha$ radiation source of wavelength 1.54 Å was used, operating in a 2θ range of 2-55º with a

scan rate of 0.5 s per step. The average *d*-spacing was obtained from the Bragg's equation:

$$n\lambda = 2d\ sin\theta \quad (2)$$

where *d* is the *d*-spacing, θ the scattering angle and *n* is an integer number related to the Bragg order.

Densities were determined from Archimedes' principle using a XS105 Dual Range Mettler Toledo balance coupled with a density kit by weighting the samples, at room temperature, in air and then in a liquid of known density (Isooctane, Sigma Aldrich, > 99%). The density of the sample was estimated from the expression:

$$\rho_{sample} = \rho_{liquid} \frac{W_{air} - W_{liquid}}{W_{air}} \quad (3)$$

The density data were used to evaluate the chain packing through the fractional free volume (FFV), which was calculated using the following relation:

$$FFV = \frac{V_e - 1.3\,V_W}{V_e} \quad (4)$$

where V_e is the polymer specific volume and V_W is the Van der Waals volume, which was given by molecular modeling applying the semi-empirical method Austin Model 1 (AM1) [31] in the Hyperchem computer program, version 8.0 [32].

Gas permeation properties were determined using the *time lag* method with a barometric permeation instrument for single gas feeds at 30 ºC. The downstream pressure was maintained below 10^{-2} mbar, while the upstream pressure was kept at 1 bar for all gases. Helium (He, 2.6 Å), oxygen (O_2, 3.46 Å), nitrogen (N_2, 3.64 Å), methane (CH_4, 3.8 Å) and carbon dioxide (CO_2, 3.3 Å), which should be the last one to avoid any influence of plasticization, were used for the permeation experiments. The purities for CH_4 and O_2 were greater than 99.95% and 99.99% for the others gases. Helium permeation tests at three upstream pressures (1, 3 and 5 bar) were carried out to ratify the absence of pinholes. Gas permeability coefficients (*P*), which are usually expressed

in Barrers [1 Barrer = 10^{-10} (cm^3 (STP) cm)/(cm^2 s cm Hg) = $7.5005 \cdot 10^{-18}$ m^2 s^2 Pa^{-1} (SI units)], were obtained from the slopes in a steady state region of pressure increment as a function of time, according to the following expression:

$$P = \frac{273}{76} \frac{Vl}{ATp_o} \frac{dp(t)}{dt} \qquad (5)$$

where *A*, *V* and *l* are the effective area, the downstream volume and the thickness of the membrane, respectively, *T* denotes the temperature of the measurement in Kelvin, p_0 refers to the pressure of the feed gas in the upstream compartment and (d*p*(*t*)/d*t*) is the rate of the pressure rise at steady state. The ideal selectivity ($\alpha_{A/B}$) for components A and B was calculated from the ratio of permeability coefficients:

$$\alpha_{A/B} = \frac{P_A}{P_B} \qquad (6)$$

where P_A and P_B are the permeability coefficients of pure gases A and B, respectively.

Mechanical properties (uniaxial tension tests) were determined on a MTS Synergie 200 apparatus fitted with a 100 N load cell at room temperature. The samples of 5 mm width and 3 cm length were clamped at both ends with an initial gauge length of 10 mm, and the elongation rate was of 5 $mm \cdot min^{-1}$. At least eight samples were tested for each film.

Computer simulation was carried out by first drawing the molecules in the desktop of Hyperchem [1] and optimizing the structures of molecules and intermediates at the AM1 level of theory [2].

Subsequently, electronic energies of the optimized geometries were calculated by Density Functional Theory (DFT) (without any geometrical constraint (use of Opt keyword) for starting molecules and final molecules) by using the Becke's three parameter hybrid functional [3] and the Lee *et al*. [4,5] correlation functional with the 6-31G(d) basis set (B3LYP/6-31G(d)). For intermediates molecules, the molecule obtained by AM1 was subsequently put to calculate by using the Gaussian 03 and

Gaussian 03W packages (6) using the energy job type (single point calculation). Additional data of the quantum-mechanical process from the conversion of ortho-huydroxypolymides to TR-PBOS and also from ortho-hydroxuypolyamides to β-TR-PBOwill be detailed in a coming work.

Semiempirical model calculations, AM1, were performed with the package implemented in Gaussion 03 and also with the AM1 package added to Hyperchem (7). The Gaussian 03 and Gaussian 03W programs packages were used for the DFT calculations throughout this work.

Molecular depicting of molecules was carried out by using the Arguslab 4.01 freeware program (8) and also with the GaussView program 5 (9).

3. Results and discussion

3.1. Synthesis and characterization of the precursor polyimides.

Precursor polyimides were synthesized by a classical and quantitative two-step low-temperature polycondensation method in which the diamine, HAB or DMAB, was combined with dianhydride 6FDA at room temperature in solution of a polar aprotic solvent (NMP or DMAc). DMAc was selected for the chemical cyclodehydration reactions due to its facility to be removed during the formation of membranes. However, in the case of azeotropic imidizations, NMP was used because the boiling temperature of DMAc is similar to that of *o*-xylene, what hinders the water release. High-viscosity poly(amic acid) intermediates, *HPAA* and *MeOPAA*, were obtained through a base-assisted *in situ* silylation method [33], which requires the use of a silylating agent (CMTS) and Py and DMAP as activating reagents to increase the reactivity of the $–NH_2$ groups. In a second stage, the poly(amic acid)s *HPAA* and

MeOPAA were cyclized by different imidization methods depending on the desired final polyimide structure.

Azeotropic imidization was carried out by adding *o*-xylene to form an azeotrope with the water produced during the ring-closure reaction. Accordingly, *HPAA* was azeotropically imidized to obtain *PI-OH* precursors.

Chemical imidizations were accomplished by the addition of a mixture of acetic anhydride and Py to the *HPAA* and *MeOPAA* solutions. Without the use of a protecting group, the hydroxyl groups of the HAB moiety were converted to acetate groups during the imidization process and thus acetate-containing polyimide, *PI-OAc*, was obtained.

PI-OH, *PI-OAc* and *PI-OMe* polyimides showed values of inherent viscosity of 1.51, 0.62 and 0.59 dL/g respectively, offering high enough molecular weight to be employed in the preparation of dense membranes with good mechanical properties. Yield of polycondensation reactions was higher than 98 - 99 % for all polyimides.

Chemical structure of precursor polyimides was confirmed by ^{1}H-NMR. Fig.1 shows the NMR spectra for the three polyimides where the peak allocations have been included. As it can be seen in the aromatic region, the hydrogens corresponding to the phenyl moieties coming from the diamine (b, c and d) are shifted upfield relative to the hydrogen peaks ascribed to phenyl groups of the dianhydride (e, f and g), which exhibited a similar chemical shift for all polymers, indicating that the influence of the electronic features of the diamine aromatic rings on the dianhydride ones was negligible. The protons of the hydroxyl phenolic group (a_1) were observed at 10.23 ppm for *PI-OH* spectrum while, in the case of *PI-OAc* and *PI-OMe* spectra, the peaks in the aliphatic region at 2.16 and 3.88 ppm corresponded to the methyl protons in the acetate group (a_2) and in the methoxide group (a_3) respectively. In addition, the absence of the

OH peak at 10.23 ppm in the *PI-OAc* spectrum indicated that whole acetylation was attained.

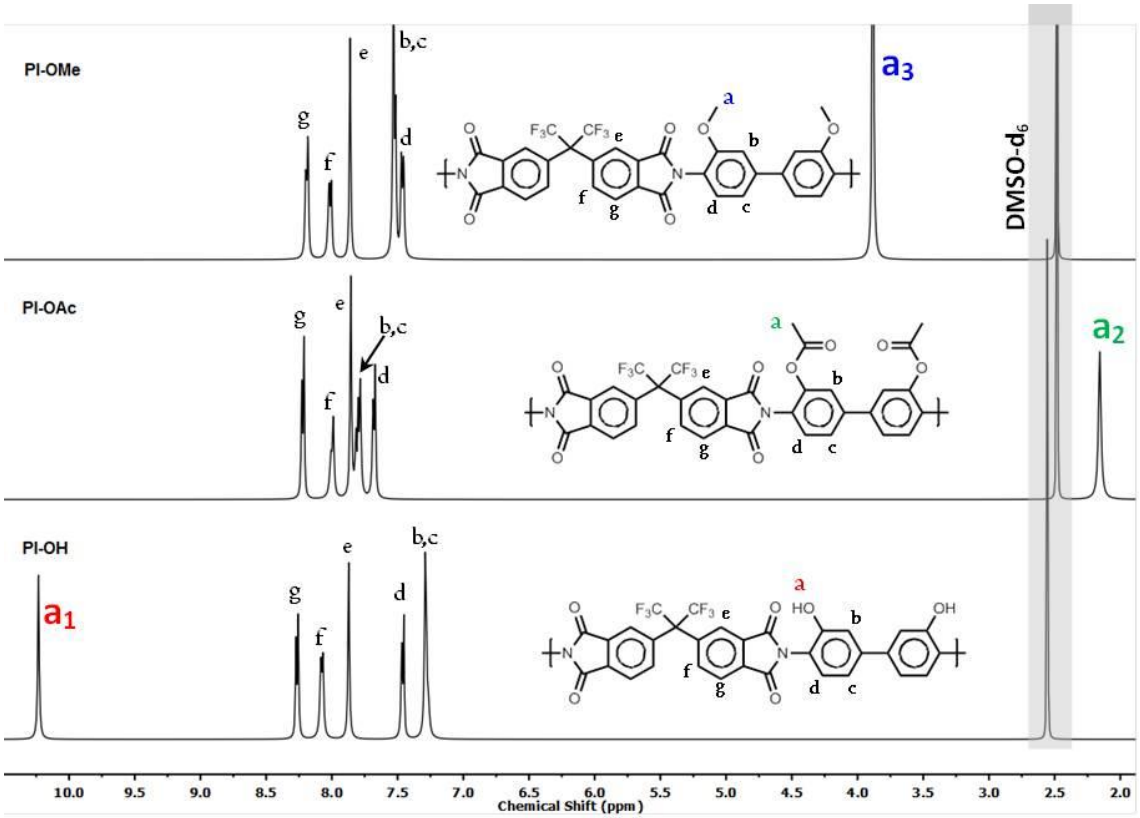

Fig. 1. ^{1}H-NMR spectra of the precursor polyimides (DMSO-d_6, 500 MHz)

The IR spectra of polyimide films are shown in Fig. 2. All polyimides showed absorption bands at around 1780 cm^{-1} (symmetric C=O stretching), 1720 cm^{-1} (asymmetric C=O stretching) and at approximately 1375 cm^{-1} (C-N stretching), ratifying the existence of imide moieties. In addition, absorption peaks at 1250 – 1100 cm^{-1} denoted the C-F stretching band of the hexafluoroisopropylidene moiety. In the case of *PI-OH* pattern, the broad band in the region of 3200 – 3600 cm^{-1} was attributed to O-H vibration of phenolic groups.

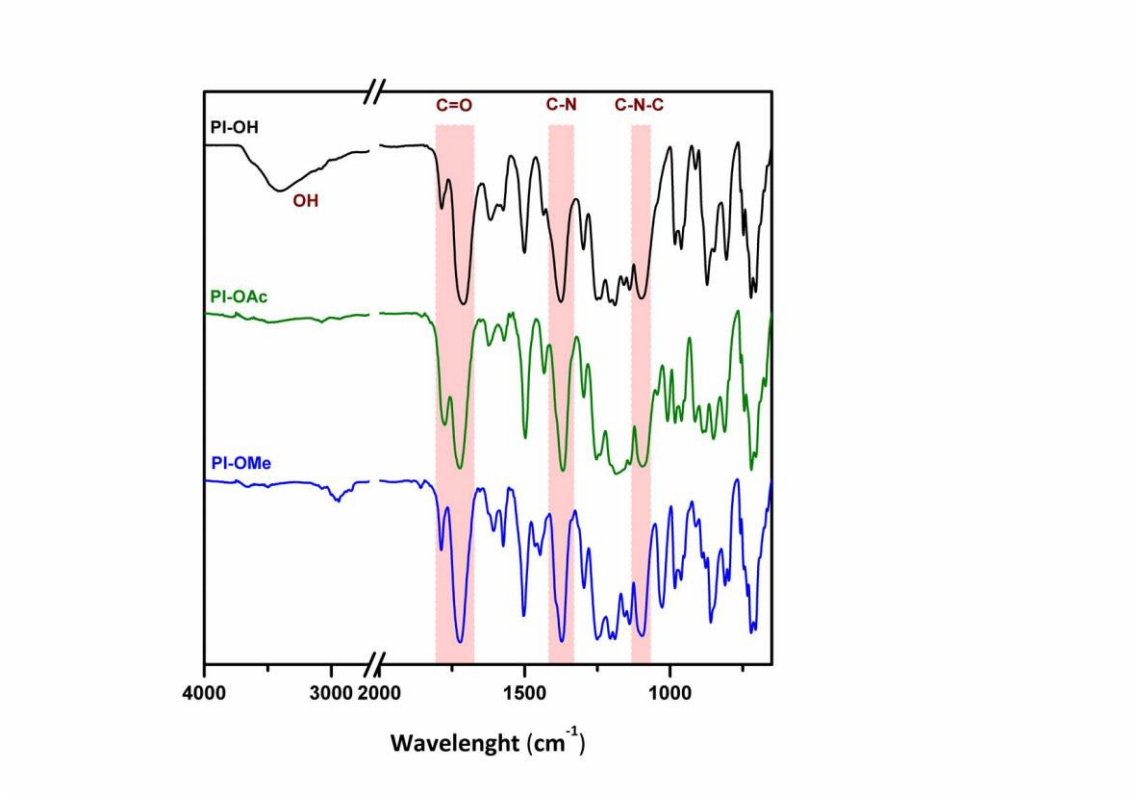

Fig. 2. ATR-FTIR spectra of precursor polyimide films.

3.2. Thermal properties of precursor polyimides.

The thermal characteristics of these three polyimides were evaluated using MDSC and TGA-MS techniques. As observed in MDSC (Fig. S1), the glass transition temperature, T_g, was clearly affected by the *ortho*-positioned substituent. Thus, the *PI-OH* exhibited the highest T_g at 356 ºC, whereas the non-hydroxylated polyimides showed a lower T_g of 278 ºC and 311 ºC for *PI-OAc* and *PI-OMe*, respectively (see Table 1). This displacement of T_g to lower values in the case of the non-hydroxylated polyimides can be attributed to the reduced ability to produce hydrogen bonds, and the higher free volume due to the presence of acetate and methoxy groups. Both factors lessen the cohesive energy and consequently the glass transition temperature.

A comparison of TGA and the first derivative traces for all precursor polyimide in form of films at 10 ºC min^{-1} under N_2 atmosphere can be seen in Fig. 3. *PI-OH* clearly shows two distinct weight loss steps, in concordance with data previously reported [30]. The first weight loss, in the range of 300-500 ºC, can be associated with the thermal rearrangement from *PI-OH* to the TR-PBO structure with releasing of CO_2, as confirmed by TGA-MS analyses (Fig. 4). The second weight loss is ascribed to the generalized decomposition of the *in situ* formed TR-PBO backbone at around 500-600 ºC. *PI-OAc* shows a similar TGA profile with two-stage weight losses as *PI-OH*, suggesting that the thermal rearrangement to TR-PBO has taken place as well in this polyimide. However, the apparent starting temperature of the first weight loss of *PI-OAc* was observed around 60 ºC lower than that of *PI-OH* (see Table 1). In addition, maximum weight loss rate (r_{max}) for *PI-OH* film, analyzed from differential TGA curve (DTG), was r_{max}=0.30%/ºC, whereas a lower value of r_{max}=0.13%/ºC was found for the *PI-OAc* film. On the other hand, it was difficult to discern the two-step weight loss for *PI-OMe* film, possibly due to the improved thermal stability given by the methoxy group or because of the existence of a different rearrangement mechanism. In this case, the apparent starting temperature for the first weight loss was observed at 380 ºC, and the maximum weight loss rate (at 495 ºC) showed a value of 0.22%/ºC.

Furthermore, the measured weight losses for the *PI-OH*, *PI-OAc* and *PI-OMe* films were 12.6, 13.0 and 13.8 %, respectively. These values are lower than the theoretical values of full conversion to PBO (correspondingly, 14.1, 24.3 and 17.8 %), on the supposition that the TR mechanism from *ortho*-substituted PI into PBO occurs in all cases. TGA-MS was used to identify the composition of the material loss from the film sample during the TGA scan. Fig. 4 shows the molecular weight of the emerged MS products between 10 and 70 amu, using the same experimental settings than those

employed in the TGA experiment illustrated in Fig. 3. In *PI-OH* film (a), components having molecular weight of 17, 18, 19, 20, 44, 51 and 69 were evolved during the full scan. As mentioned above, the first mass loss is attributed to decarboxylation of the polyimide during thermal rearrangement; thus, just the peak associated with the molecular weight 44 was observed below 450 ºC. In the second stage, which is associated with polymer degradation, molecular weight species of 17, 18, 19, 20, 44, 51 and 69 were detected. MS losses of 19, 20 and 69, indicate the cleavage of the groups having fluorine atoms (trifluoromethyl) on the polymer backbone, corresponding to fragments of F, HF and CF_3, respectively. The peaks associated to molecular weights of 17 and 18 reveal a loss of water of the polyimide structure. Finally, molecular weight losses of 44 and 51 can be attributed to the polyimide general degradation. However, for the *PI-OAc* film, in addition to these molecular losses, other peaks can be observed in the thermal rearrangement region. Thus, mass loss related with molecular weights 41 and 42 were attributed to loss of the acetate groups in form of a ketene moiety. Moreover, molecular weights of 17 and 18, corresponding to H_2O, were also detected in the first step, which could plausibly indicate that chemical imidization was not complete in this case. In *PI-OMe*, in the first weight loss region, along with the peak associated to CO_2, a weak change in intensity was observed for specie having a molecular weight of 15, which could be associated to loss of methyl groups coming from the methoxy group breakage.

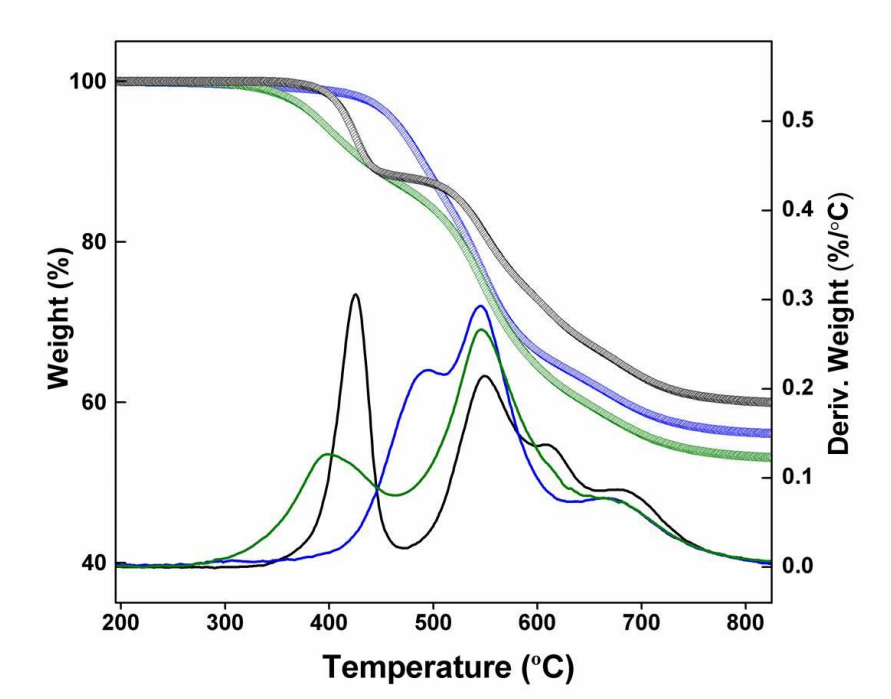

Fig. 3. Thermogravimetric analysis of precursor polyimide films at a heating rate of 10 ^{o}C min^{-1} under N_2 atmosphere; ● *PI-OH*, ● *PI-OAc* and ● *PI-OMe*.

Table 1. Thermal properties of precursor polyimide films.

Polymer code	T_g (°C)[a]	T_{AP} (°C)[b]	T_{Max} (°C)[c,d]	Theoretical wt. loss (%)	Measured wt. loss (%)[d]	T_d (°C)[d]
PI-OH	356	345	425	14.1	12.6	550
PI-OAc	278	282	397	24.3	13.0	546
PI-OMe	311	380	493	17.8	13.8	546

[a] Middle point of the endothermic step of the "reversing" contribution to the average heat flow during the first scan of MDSC measurements conducted with a heating rate of 5 °C/min and a modulation period of 40 s and amplitude of the temperature modulation of 1.5 °C, under a nitrogen atmosphere. [b] Apparent starting temperature at which first weight loss begins. [c] Temperature at the maximum point of first weight loss. [d] Determined by TGA at a heating rate of 10°C/min under nitrogen atmosphere.

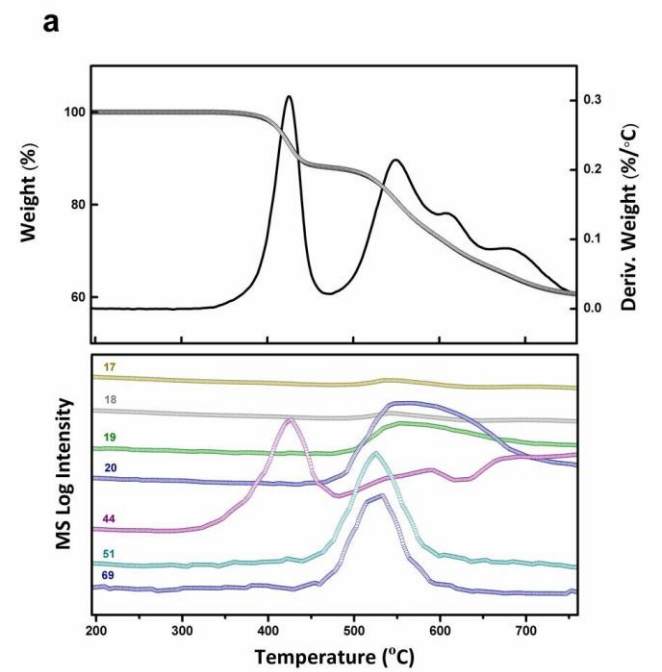
a
Weight (%)
Deriv. Weight (%/°C)
MS Log Intensity
17
18
19
20
44
51
69
Temperature (°C)

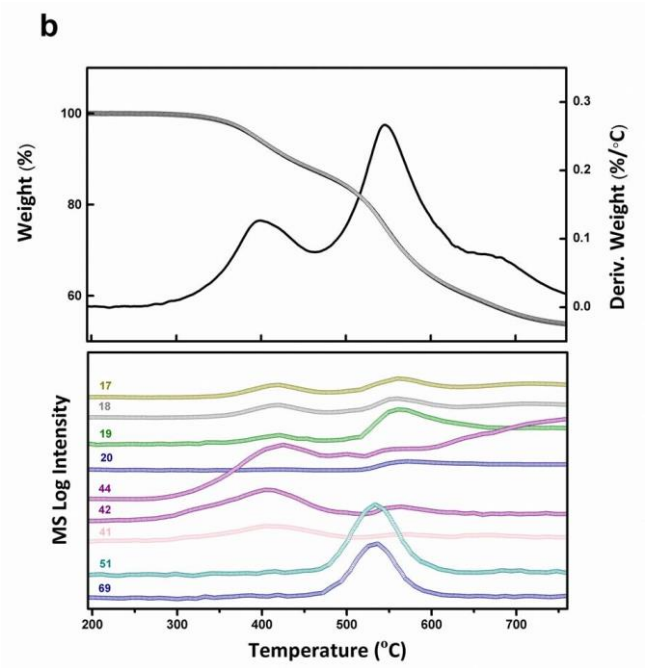
b
Weight (%)
Deriv. Weight (%/°C)
MS Log Intensity
17
18
19
20
44
42
41
51
69
Temperature (°C)

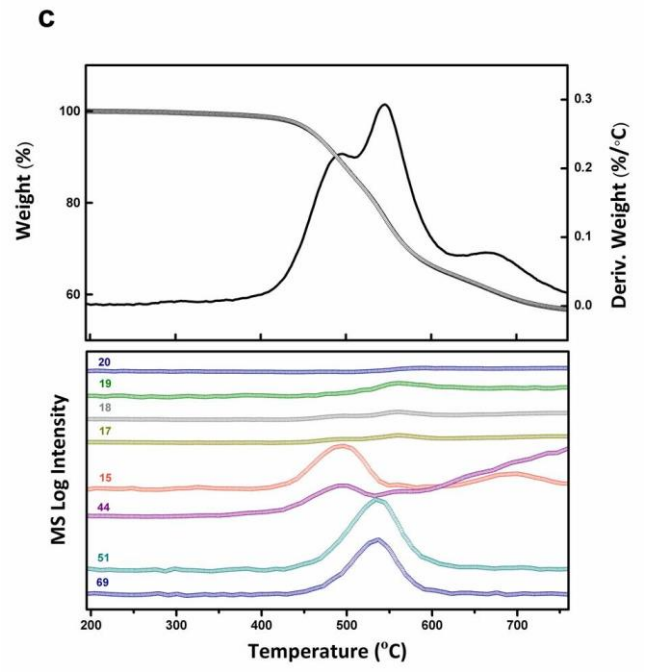

Fig. 4. Thermogravimetric analysis combined with mass spectroscopy (TGA-MS) of (a) *PI-OH*, (b) *PI-OAc* and (c) *PI-OMe* precursor polyimide membranes (heating rate of 10 $^{o}Cmin^{-1}$ under N_2 atmosphere).

3.3. Thermal treatment of precursor polyimides.

Supplementary TGA analyses were performed to adjust the thermal treatment settings for TR sample preparation in the tubular furnace. Thus, the PI films treated at 300 ºC were further heated to the desired temperature (350 ºC, 400 ºC and 450 ºC) using a heating rate of 5 ºC min^{-1}, and held isothermally at the target temperature for 3h. Fig. 5 depicts the isothermal thermograms for *PI-OH*, *PI-OAc* and *PI-OMe* precursor films, representing weight loss as a function of time after reaching the desired rearrangement temperature.

The conversion percentage of the precursor polyimide films into the assumed final TR membranes was evaluated based on data obtained from isothermal thermograms using Eq. (7):

$$\%\, Conversion = \frac{Experimental\ Mass\ Loss}{Theoretical\ Mass\ Loss} \times 100 \quad (7)$$

This theoretical CO_2 loss, which is 14.1 % for *PI-OH*, 24.3 % for *PI-OAc* and 17.8 % for *PI-OMe*, is shown as a dashed line in the figure.

Conversion values for the precursors polyimides are collected in Table 2. According to previous studies [30,34,35] the thermal cyclization reaction is very sensitive to the applied temperature, showing an acceleration in the thermal rearrangement kinetics on increasing temperature.

As it can be seen, the amount of weight loss increases as a function of rearrangement temperature and time, for all cases. For *PI-OH* film, at 350 ºC, the weight loss was very low for any heating time (11 %), whereas it notably increased at 400 ºC reaching the maximum value (96 %) at 450 ºC, exceeding the theoretical weight loss for long treatment times. However, at 350 ºC, *PI-OAc* film achieved higher weight loss than *PI-OH*, (33 %) presumably due to its lower T_g, that favors the start of rearrangement at a lower temperature, as it has been seen in Fig. 3. At 400 ºC and 450 ºC, the weight loss gradually increased, probably reaching the theoretical value for treatments longer than 3 h at 450 ºC. In the case of *PI-OMe*, the weight loss was very low for any heating time both at 350 (4 %) and at 400 ºC. As the T_g of this polymer is also significantly lower than that of *PI-OH*, the lower reactivity of this PI should be related with the different behavior of the OMe group, as it has been indicated above for the dynamic TGA curves. At 450 ºC, in the manner of *PI-OH* film, the weight loss

notably increased but in this case, the value did not surpass the theoretical weight loss for the first 3 h (61%). Presumably, using a longer thermal treatment would result in a higher percentage of conversion and, consequently, higher d-spacing values, which would translate into a higher degree of *openness* of the polymer matrix.

In order to have thermal histories similar to those reported in other studies related with TR materials, the residence times chosen for thermal treatment were 1 h for 350 ºC and 400 ºC, and 30 minutes for 450 ºC (represented by empty circles in the Fig. 5). Thus, the polyimide precursors, *PI-OH*, *PI-OAc* and *PI-OMe*, were thermally treated in a tubular furnace following the chosen protocols.

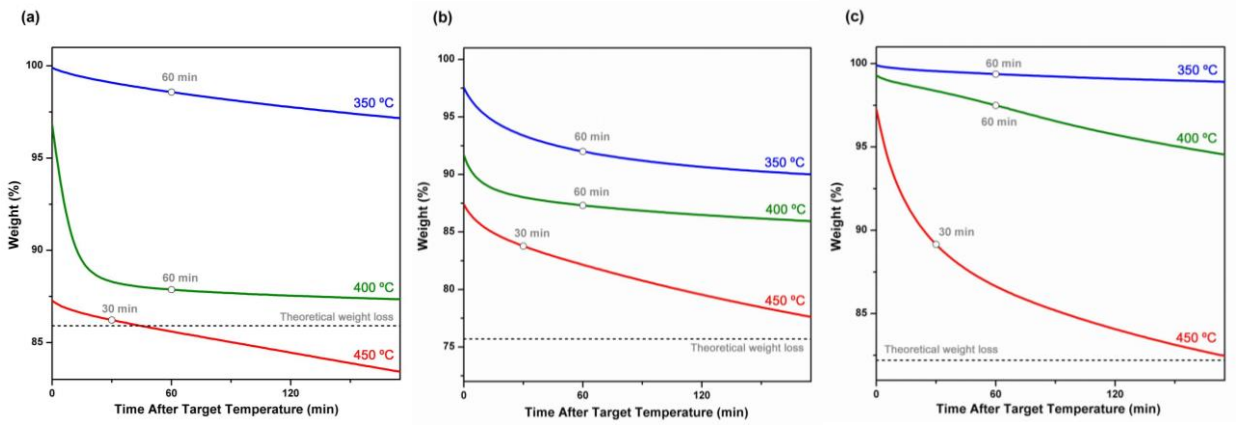

Fig. 5. Isothermal thermogravimetric analysis, under N_2 atmosphere, of (a) PI-OH, (b) PI-OAc and (c) PI-OMe precursors. This graph shows weight loss of these polyimides as a function of time at the indicated temperatures. Empty circles represent the conditions used for membranes employed in transport property characterization.

The effect of the thermal treatment on polymer chain packing, which has a considerable influence on the gas separation properties, was explored by wide-angle X-

ray diffraction (WAXD). In Fig. S2, the X-ray patterns, measured at room temperature, of thermally treated membranes and polyimide precursor films are compared. All of the membranes were in a completely amorphous state, proved by the presence of an amorphous halo. The most probable intersegmental distance (d-spacing) values were estimated according to Bragg's equation, and data are collected in Table 2.

The precursor polyimides, *PI-OH*, *PI-OAc* and *PI-OMe*, showed preferential intersegmental distances with values of 5.57, 6.11 and 5.99 Å, respectively, whereas films treated at 450 ºC resulted in a larger intersegmental distances, with values of 6.14, 6.51 and 6.36 Å, respectively. For the other treatments, a rather linear change was observed. Accordingly, the use of thermal treatment led to lower chain packing densities, which was in agreement with other TR polymers previously reported [30,34,36].

Table 2.

Polymer code	Conversion[a] (%)	Density (g cm^{-3})	FFV	Increment in FFV (%)	d-spacing (Å)
PI-OH	0	1.458	0.160	–	5.57
TR-OH350	11	1.453	0.159	–	5.71
TR-OH400	86	1.373	0.176	10	6.06
TR-OH450	96	1.337	0.194	21	6.14
PI-OAc	0	1.413	0.170	–	6.11
TR-OAc350	33	1.429	0.154	–	6.05
TR-OAc400	52	1.391	0.172	1	6.30
TR-OAc450	67	1.345	0.196	15	6.51
PI-OMe	0	1.388	0.174	–	5.99
TR-OMe350	4	1.376	0.181	4	6.16
TR-OMe400	14	1.360	0.191	10	6.20
TR-OMe450	61	1.322	0.214	23	6.36

[a]PI transformation for the different series after 60 min at 350 and 400 ˚C and 30 min at 450 ˚C

The density of the precursor polyimide films and the thermally treated films was measured in a density balance from the difference of the specimen weighed in air and in isooctane. Density data are also compiled in Table 2. It was observed that the density of

the polyimide precursor films was higher for *PI-OH* due to its ability of creating hydrogen bonds, which gave rise to a more densely packed polyimide structure. As expected, thermally treated membranes showed lower densities as thermal treatment temperature was further increased, excluding TR-OAc350 membrane which showed slightly higher density than its precursor membrane, *PI-OAc*.

The density values were used to evaluate the fractional free volume (FFV) of precursors and thermally treated films using Eq. (8), where V_o is commonly referred to as the occupied volume of the polymer chain and V_e is the specific volume, which is the inverse of the polymer density.

$$FFV = \frac{V_e - V_o}{V_e} \quad (8)$$

These volumes were calculated according to the Bondi's group contribution theory using Eq. (9), where V_W is the van der Waals volume. The Van der Waals volumes, V_W for partially converted samples were calculated applying Eq. (10), which considers the degree of conversion of the polyimide precursor into the final TR structure; and *c* is the fractional mass conversion determined as the quotient of the experimental mass loss measured by TGA and the theoretical mass loss to achieve virtual 100 % conversion (Eq. (7)). $V_{W,TR}$ and $V_{W,PI}$ values refer to the Van der Waals volume of TR and PI structures, respectively.

$$V_0 = 1.3 \sum V_W \quad (9)$$

$$V_W = c\, V_{W,TR} + (1 - c) V_{W,PI} \quad (10)$$

The changes occurred in the structure of the precursor polyimides after thermal treatment in the furnace were controlled using ATR-FTIR analysis. A complete monitoring of these structural changes can be seen in Fig. S3, where the ATR-FTIR spectral results for all thermally treated samples as well as for polyimide precursors are illustrated. Fig. 6 shows the ATR-FTIR spectra of the films thermally treated at the highest temperature (450 ºC) for 30 minutes.

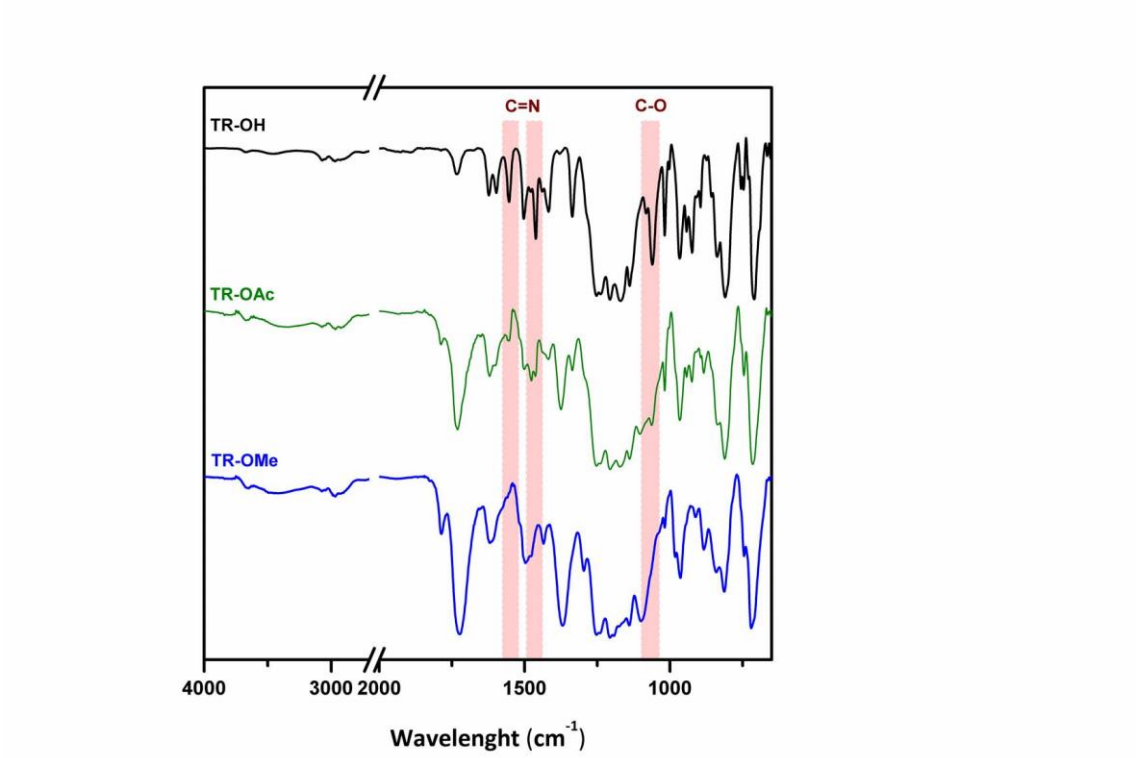

Fig. 6. ATR-FTIR spectra of films thermally treated at 450 ºC during 30 minutes

As can be seen, in TR-OH sample spectrum, the appearance of intense peaks at wavenumbers around 1557, 1465 and 1060 cm^{-1}, which are characteristic of the PBO structure, ratified that *PI-OH* film undergoes a thermal rearrangement into PBO. In addition, the intensity of the imide peaks at 1780, 1720, 1375 and 1102 cm^{-1}, and the strong and broad absorption band from hydroxyl group around 3400 cm^{-1}, substantially decreased. In TR-OAc spectrum, the representative peaks of PBO could also be

observed, even though they were less intense when compared with TR-OH sample, evidencing the existence of PBO in the final structure. In this case, the imide peaks partially decreased, and the emergence of a new strong band around 3400 cm^{-1}, which did not appear on the spectrum of the *PI-OAc* precursor, proved the presence of new OH phenolic groups. In the case of TR-OMe, it could also be seen the appearance of the characteristic peak of OH phenolic group and a low decrease of the imide peaks. However, as mentioned above, the polymer density decreased also in this case from the starting material to the final one, which permits to presume that a structural change took rise, similar to that undergone by *ortho*-hydroxypolyimides. It is well documented that pyrolysis of methoxy aromatic compounds proceeds via the homolytic scission of the (H_3C)-O linkage, with the subsequent loss of CH_3 as methane or ethane and recombination of the phenoxy radical to phenol [37]. If this mechanism is accepted as a first step of the transformation, *ortho*-methoxypolyimides would then render TR-PBOs in the same way as *ortho*-hydroxypolyimides do. Yet, the identification of the final material, TR-OMe450, by FT-IR did not entirely agree with this assumption as a clear transformation into PBO was not confirmed by the spectra at all. As commented above, the strong carbonyl bands of imide C=O stretching at around 1715 and 1785 cm^{-1} persisted in great extent after heating at 450 °C for 30 minutes, contrarily to what happens on heating *ortho*-hydroxypolyimides, and that seems contradictory with the proposal that the most probable first step of the thermal treatment is the loss of methyl groups with subsequent formation of phenols or phenol radicals, that is, with almost simultaneous formation of *ortho*-hydroxypolyimide. Thus, the persistence of the intense imide peaks and the non-appearance of the characteristics PBO bands seemed to evidence that the thermal rearrangement did not occur via the accepted *TR-PBO* process.

These spectroscopic evidences moved us to look for a plausible route that makes clear the mechanism governing the thermal rearrangement undergone by the current *ortho*-methoxypolyimides. If one makes a conscientious revision of spectral data reported for TR-PBOs in last years, two points appear as most significant: 1) there is a general agreement to accept the mechanism proposed by Tullos *et al.* for the thermal rearrangement of *ortho*-hydroxypolyimides to TR-PBOs [24,38–42], although there is not full agreement about the effect of the precursor synthesis route (chemical imidization, azeotropical imidization or direct thermal imidization or even on the final products formed during the thermal treatment) on the composition of the final TR-PBO [36,41–45], and 2) when starting from *ortho*-esterpolyimides the composition of the final material is far from being a neat PBO as strong spectral evidences speak for the prevalence of polyimide in great extension [40]. In fact, if one revises the attempts made to use *ortho*-esterpolyimides (mainly *ortho*-acetylpolyimides) instead of *ortho*-hydroxypolyimides as precursors of TR-PBOs, it can be noticed that the possibility of an alternative mechanism was obviated, authors focusing their research effort mainly on studying the advantages of using *ortho*-esters in terms of a better solubility, improved FFV (as the splitting off of aliphatic rests should help for an increase of regular microcavities) or a lower T_g, which could favor a drop of the rearrangement temperature. But, as a rule, the final heated films of supposed TR-PBOs exhibited strong IR bands corresponding to aromatic imides, and authors have not paid special attention to this experimental evidence. Thus, another mechanism, or a parallel one, could be responsible for the final chemical composition shown by IR spectra in those cases where *ortho*-hydroxypolyimide is not the precursor.

Kostina *et al*. have recently reported a thorough study addressed to make clear the mechanisms that govern the molecular transformations undergone by *ortho*-

hydroxypolyimides at temperatures over 400 ºC [26,46]. They have postulated that the formation of rigid cyclolactams, and not only polybenzoxazoles, is responsible of the chain conformational changes which lead to the observed strong effects on physical properties, and particularly to the dramatic increase of fractional free volume and hence of gas diffusivity. In those papers, and based on spectroscopic signals, the observed loss of CO_2 was ascribed to the formation of lactams through thermal decomposition of a cyclic intermediate amide-ester. This assumption was supported by quantum chemical calculations, which suggested that the formation of lactams was energetically more favorable than the formation of benzoxazoles. Nonetheless, it can be presumed that by applying the very high temperatures used to force the intramolecular rearrangement, both lactams and benzoxazoles could be formed, and that the final composition is greatly affected by the final temperature and the heating protocol. In this regard, it is to remark that there is a spectroscopic indication of polyimide persistence, apart from the merging of bands attributable to lactams, as the characteristic IR bands of imide at about 1778, 1720, 1550 and 725 cm^{-1} remained in the IR spectra reported by Kostina *et al*, and that is so also for most of the TR-PBOs prepared from *ortho*-esterpolyimides reported until now [26,46].

Thus, it seems that, although *ortho*-hydroxypolyimides do lead mostly to TR-PBOs by thermal rearrangement, heating other related precursors, as *ortho*-esterpolyimides or *ortho*-methoxypolyimides, does not give the same rearrangement paths and the resulting material after heating up to 450 ºC is far from being neat polybenzoxazole. The presence of cyclolactam, cyclolactam-ester and benzoxazole can be detected in varied proportion depending on: 1) the nature of the precursor, 2) the synthetic method applied to prepare the precursor and 3) the schedule followed in the final heating step. Furthermore, in the particular case of TR polymers attained from

ortho-methoxypolyimide, benzoxazole units should be present in a very small proportion as spectral data do not support their presence in significant amount.

So, a mechanistic path is proposed in this paper to figure out the process involved in the thermal treatment at high temperatures in solid state of *ortho*-methoxypolyimides. This mechanistic explanation is far from being thoroughly justified and additional work in this topic will be carried out by using other techniques as solid-NMR, XPS and FTIR-MS for models obtained in a regioselective way and it will be published in a near future.

Based on the work related in TR materials, the mechanistic path would be described by Scheme 2.

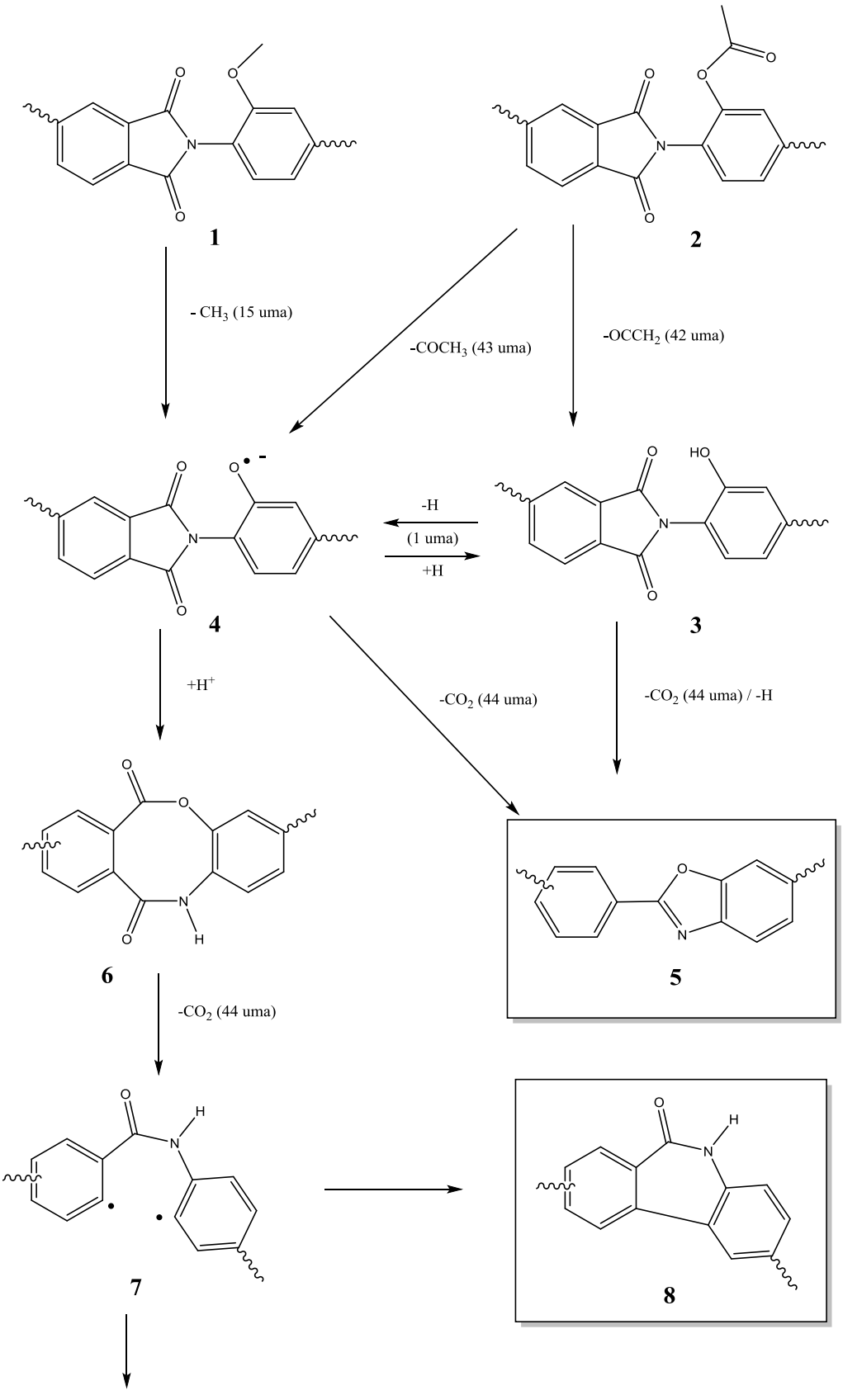

Scheme 2. Possible rearrangement mechanisms and final reaction products obtained by thermal treatment of *ortho*-hydroxy, *ortho*-methoxy and *ortho*-acetyl polyimides.

We postulate that the final molecular moieties arising from the thermal treatment depend on the group attached on the *ortho* position of the amino group. By simplicity sake, the employed groups in this description were OH, methoxy and acetyl ones. When the group is OH (3), the high temperature produces the conversion to TR-PBO (5) or the formation of (4) by homolytic breakage of the O-H bond. When acetyl group (2) is considered a predominant loss of ethenone (ketene, CH_2=C=O) is observed, as evidenced by TGA-MS, with formation of (3 or 4). This group (m+=42) is formed by decomposition of the –(OCO) bond with formation of the acyl group and breakage of this group to ethenone and a proton. However, when the methoxy group is considered, TGA-MS denotes the loss of methyl groups (m+=15 uma), which produces the formation of (4).

When acetyl group (2) is considered, a predominant loss of ethenone (ketene, CH2=C=O) is observed by TGA-MS, with formation of (3). This group (m+=42) is formed by decomposition of the –(OCO) bond with formation of the acyl group and breakage of this group to ethenone and a proton. However, when the methoxy group is considered, TGA-MS denotes the loss of methyl groups (m+=15 uma), which produces the formation of (4). Evidently, 3 can be converted to 4 and 4 to 3 by loosing or gaining an H, respectively.

Obviously, the published works and the results of this one clearly point that the formation of the benzoxazole moiety is most favored by the OH precursor, slightly favored for the $OCOCH_3$ precursor, and less favored by the precursor having the methoxy group.

Therefore, it could be assumed that the presence of H (H+ or H·) in the medium will influence the rearrangement process. When the amount of H is high (OH polyimide), the classical TR rearrangement is very clear and the benzoxazole moiety formation is

evident. However, the production of H groups is very small when the methoxy group is considered and the PBO formation is scarcer. For the acetyl polyimide, mixed formation of both (3) and (4) intermediates could explain the observed FTIR results.

Two questions arise from this assumption: 1) which is the role of H in the PBO formation? and 2) why the formation of non-PBO moieties (mainly for methoxy PI and in a relatively high amount for acetyl PIs) produces materials with high FFV and very high gas diffusivities?

1) The role of the proton could be ascribed to the protonation of any nucleophilic group, which could produce an intermediate state that permits the formation of any molecular moiety described in the Scheme 2.

It seems to be accepted in the bibliography that the intermediate moiety formed during the conversion from *ortho*-hydroxypolyimide to polybenzoxazole is the B molecule described in Scheme 3.

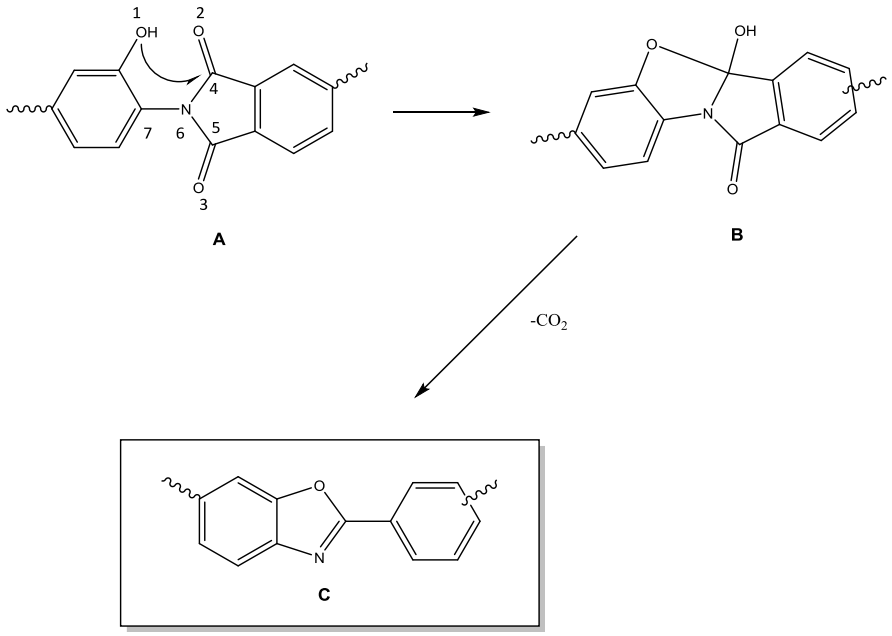

Scheme 3. Reaction mechanism proposed by the thermal rearrangement mechanism of PI-OH to TR-PBO

The formation of the intermediate B seems to be evident, and hence many authors consider this moiety to be the essential one to achieve the final benzoxazole. However, a molecular simulation study denotes that the distance from the nucleophilic center (O1 of the OH moiety after the breakage of the O-H bond) to the carbonylic centers of the imide (C4 or C5) is rather larger than 2.8 A and a very strong conformational change has to take place to make possible this attack.

However, it is plausible to consider that, at this high temperature, a proton is able to jump from the OH to any of the nucleophilic centers of the imide (see Scheme 4). When one of the two oxygens of the imide group is protonated (structures D and E) an increase of the energy of the molecule is observed. However, no changes in the distance between the O1 and the carbonylic center C4 or C5 are observed (the lowest possible value for an eclipsed conformation is higher than 2.7 A) and consequently the geometry of the protonated molecule does not favors the attack to the carbonylic centers. Nevertheless, when the proton attacks the nitrogen of the imide group an important conformational change takes place and the nitrogen adopts a pyramidal (sp^3) conformation. As a consequence of the new nitrogen conformation, the distance from O1 to C4 or C5 is significantly shortened (the shortest possible distance is 2.00 Å) in such a way that the attack is possible.

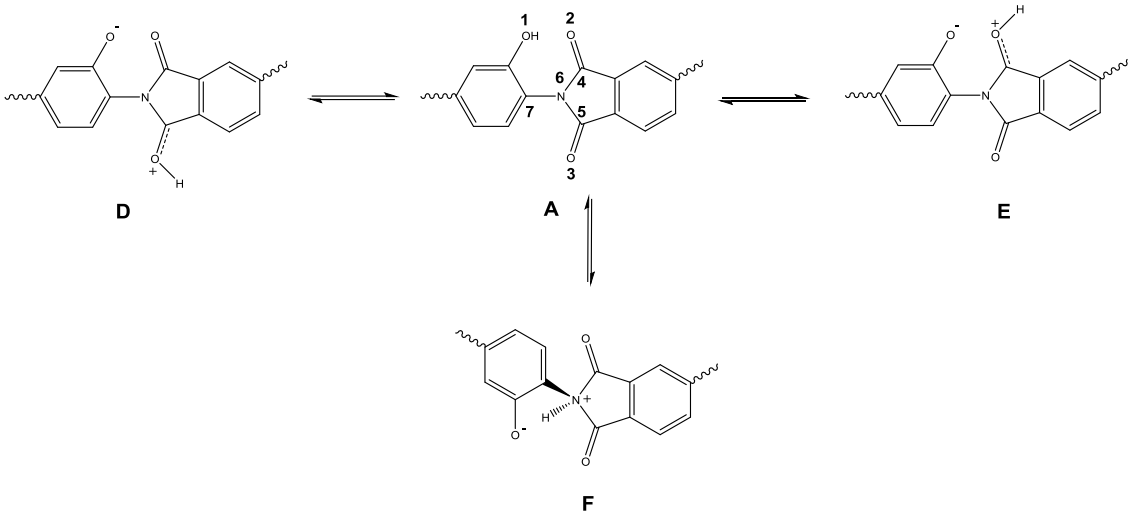

Scheme 4. Proton jumping between PI-OH and the different nucleophilic centers of the imide moiety

Fig. JJ depicts the structure of the protonated intermediate F showing the shortest distance between O1 and C4 or C5 that can be attained when the structure is allowed to rotate around the bond N6-C7.

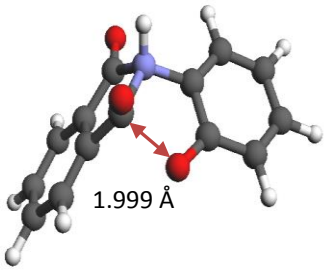

Fig. JJ. Structure of the *ortho*-hydroxypolyimide after the transfer of one proton from the OH group to the nitrogen imide moiety, showing the involved conformational change and the significant shortening of the distance between O1 and C4 or C5.

Afterwards, the system evolves to the formation of the benzoxazole groups through the jumping of the hydrogen placed on N6 to the O2, thus forming the bicyclic intermediate state (Fig. BB).

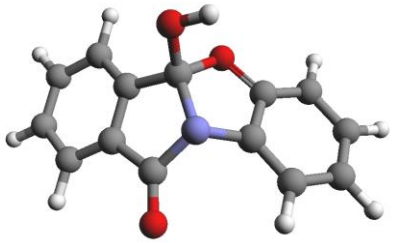

Fig. BB. Intermediate molecule B formed from intermediate B

Additional protonation of O2 on BB, produces the releasing of a water molecule by breaking of the bond O2-C4,. Additional reaction of the water molecule on C5 gives the 2-carboxy benzoxazole that, by losing a CO_2 molecule is converted, at this temperature, to the final benzoxazole.

However, when no hydrogens (protons (H+) or hydrogen radicals ($H^{\cdot}$)) are involved in the reaction, several steps of the proposed mechanism are not possible. However, the reaction progresses by thermal activation of the primary conformation. Thus, the eclipsed conformation of F can be achieved by rotation of the N6-C7 bond, favored by the high temperature, as it has been commented above, permits the attack of O1 to C4, and the system evolves spontaneously to the formation of the cycloester-lactam moiety. This spontaneous reaction, which is shown in Fig. CC, has been seen by computer simulation, by using the semiempirical AM1 method. In fact, if the structure in Fig. JJ is minimized by AM1, it spontaneously gives way to the cyclo-ester lactam

The ulterior decarboxylation of the cyclo-ester lactam forms the proposed lactam. However this decarboxylation also produces a high amount of radical centers, which lead to a massive amount of crosslinking.

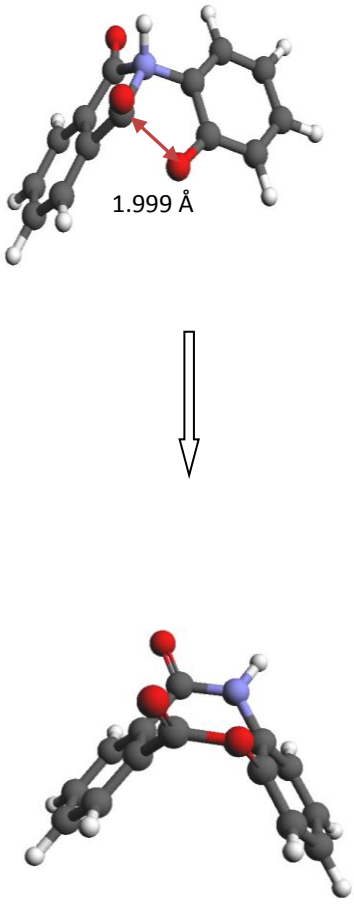

Fig. CC. Initial and final steps of the reaction of evolution of intermediate F to cycloester-lactam when there is no protonation of O2 atom.

2) The high FFV of the materials made from *ortho*-methoxypolyimides can be explained by the eclipsed and bent conformation associated to the transitory molecule needed to produce the attack. Also, the cycloester lactam has a very contorted conformation that should introduce an important amount of free volume excess.

3.4. Mechanical properties

Mechanical properties were determined for all polymeric films of this research work (precursor and thermally treated materials) and are shown in Table 3.

Mechanical properties for precursors were excellent with elastic moduli above 2.5 GPa, tensile strength higher than 150 MPa and good values of elongation to break. The mechanical properties for the membranes thermally treated at 350 ºC did not appreciable change, except for the *PI-OAc* membranes, probably due to a premature thermal rearrangement as it was observed by thermogravimetric analysis. The thermal treatment at 400 ºC led to a slight decrease of mechanical properties, which was higher for the membrane derived from *PI-OAc*. However, the membranes from *PI-OMe* and *PI-OH* showed competitive mechanical properties when compared with other aromatic polymers. It should be noted out, at this point, that it lacks a detailed study of mechanical properties for TR materials and only a few papers have dealt with this issue. Thus, Calle et al [35] obtained TR derived from ether-benzoxazole units that showed mechanical properties rather lower than these obtained in this work for the samples thermally treated at 400 ºC. Li et al [47] developed a class of TR with excellent mechanical properties, but the precursor had a high FFV and the conformational changes associated to the thermal rearrangement were favored and it was found that elongation values were clearly higher than for any TR materials obtained so far.

The mechanical properties for the samples treated at 450 ºC dropped in all cases, and lessening of 25-40 % were observed for mechanic moduli a. However, the decrease in tensile strength was significantly higher, with decreases between 70 and 80 % when compared with the reference polyimides Again, and as it is common for TR materials, the elongation values were lower than 5 %.

In particular, the best mechanical properties balance for these materials corresponded to TR-OMe450. In conclusion, it could be stated that the thermal treatment of TR membranes from *PI-OMe* gave materials with mechanical properties able to withstand the high pressures employed in industrial gas separation applications.

Table 3. Mechanical properties of precursor polyimide films and their corresponding thermally treated membranes

Polymer code	Tensile strength (MPa)	Elongation at break (%)	Modulus (GPa)
PI-OH	166	19.5	2.5
TR-OH350	167	15.9	2.7
TR-OH400	127	14.4	1.8
TR-OH450	27	1.7	1.8
PI-OAc	169	9.8	2.9
TR-OAc350	126	5.3	3.0
TR-OAc400	64	2.8	2.8
TR-OAc450	33	1.9	2.1
PI-OMe	176	7.5	3.0
TR-OMe350	179	8.8	2.7
TR-OMe400	146	8.7	2.3
TR-OMe450	56	3.6	1.8

3.5. Permeation properties

Gas transport properties of the current *ortho*-substituted polyimides and their corresponding TR-polymers were investigated for He, O_2, N_2, CO_2 and CH_4. The gas transport measured on the untreated precursor presented values of permeability which can be taken as acceptable, considering the linearity of the polymer and its chemical composition; for instance, permeabilities found for the tested gases compared well with those of the technical polyimide Matrimid®, which is commonly taken as a reference.

As can be observed in Table 4, up to 350 ºC, the changes observed in the polymer structure did not greatly affect the permeation properties, but a sudden, intense increase of permeability for all the gases tested occurred over 400 ºC, with a maximum at 450

ºC, just around the limit of thermal resistance of aromatic polyimides. As can be seen, the thermal rearrangement caused the highest increment for the acetoxypolyimide (*PI-OAc*) and the lowest one for the hydroxypolyimide (*PI-OH*), while the gain in permeability for the methoxypolyimide lied in the middle, with permeability for CO_2 27 times higher than that of the precursor *PI-OMe* and about 23 times higher for O_2.

As can be seen on comparing the FFV of *PI-OAc* and *PI-OMe*, there is a correlation between free volume and gas transport as the former has a lower FFV than the latter and the permeabilities experimentally found were lower for *PI-OAc* than those of *PI-OMe*. However, heating over 400 ºC brought about an inversion of this trend as from this temperature on and up to 450 ºC the gas permeability of *PI-OAc* rose much faster than that of *PI-OMe*. The acetyl group is considerably bigger than the methoxy one and over 400 ºC the loss of acetyl groups should leave larger elements of free volume than those left by the splitting off of methyl groups. Therefore, the rapid increase of permeability observed in *PI-OAc* from 350-400 ºC and up to 450 ºC respect to *PI-OMe*, should be ascribed to the loss of a bigger substituent and to a greater extension of rearrangement into lactam and PBO.

Table 4. Gas permeation properties of precursor polyimides and thermally treated membranes.

Polymer code	Permeabilities (Barrers)[a]					Ideal Selectivities[b]	
	PHe	P_{N_2}	P_{O_2}	P_{CH_4}	P_{CO_2}	$\alpha_{O2/N2}$	$\alpha_{CO2/CH4}$
PI-OH	46	0.35	2.3	0.16	10	6.6	63
TR-OH350	70	0.59	3.8	0.29	16	6.4	55
TR-OH400	94	2.3	12	1.5	57	5.2	38
TR-OH450	200	10	45	7.7	240	4.5	31
PI-OAc	43	0.44	2.5	0.2	12	5.7	60
TR-OAc350	75	1.1	6.1	0.48	27	5.5	57
TR-OAc400	178	5.9	29	3.2	159	4.9	50
TR-OAc450	348	28	114	21	632	4.1	31
PI-OMe	56	0.68	4.1	0.31	20	6.0	65
TR-OMe350	75	1.1	6.1	0.48	28	5.5	58
TR-OMe400	118	3.0	14	1.6	78	4.7	49
TR-OMe450	328	23	93	18	540	4.0	30

[a] 1 Barrer = 10^{-10} cm^3 (STP) cm / (cm^2 s cm Hg), measured at 1 bar , 30 ºC. [b] Ideal selectivities were obtained by the ratio of two gas permeabilities.

4. Conclusions

Ortho-methoxypolyimides were successfully synthesized from 2,2´-dimethoxybenzidine and dianhydride 6FDA. Their treatment at high temperature, up to 450 ºC, led to insoluble materials, whose IR spectra indicated a change of the chemical composition. Significant changes of the physical properties, particularly a dramatic change of the permeation properties were also observed

FTIR and TGA combined with Mass spectrometry confirmed that methoxy groups were lost in a first step that started above 350 ºC, and that a thermal rearrangement took rise at higher temperature. Unlike *ortho*-hydroxypolyimides, *ortho*-methoxypolyimides did not seem to be converted into PBOs but the starting polyimide remained in a great proportion along with the formation of benzoxazole and cyclolactam units. Benzoxazoles and cyclolactams appeared as a result of intramolecular recombination that can occur simultaneously at very high temperature. This could not be quantitatively evaluated by FT-IR. Thus, there is still a lack of knowledge about the actual mechanism that governs the path from *PI-OMe* to TR polymers. In this work, based on the accepted mechanistic paths and also on some papers published recently, a plausible molecular

simulation justification is proposed. In this explanation, the presence of protons or radical hydrogen atoms plays a critical role on the feasibility of benzoxazole formation. Also, the formation of cycloester-lactam or lactam moieties could be justified.

Then, it is reasonable to presume that, at the extreme temperatures applied for the conversion, more than one rearrangement or recombination are possible, which lead to a final material that contains polyimide and moieties of lactam and benzoxazole.

The permeation properties of the TR polymers reported here are very attractive and they compare fairly well with those of TR-PBOs previously reported, exhibiting P(CO_2) up to 540 Barrers and selectivities of 4.0 and 30 for the pairs O_2/N_2 and CO_2/CH_4, respectively. Additionally, the monomer dimethoxybenzidine used in this work is easily available and PI-OMe show better stability and handling ability than PI-OH, which make these methoxy-substituted polyimides suitable candidates for the technical development of high efficiency gas membranes.

Acknowledgments.

The financial support provided, by the MINECO (MAT2011-25513, MAT2010-20668, MAT2013-45071-R and CTQ2012-31076). This research was also supported by the Korea Carbon Capture & Sequestration R&D Center (KCRC) through the National Research Foundation of Korea (NRF) funded by the Ministry of Science, ICT, and Future Planning (NRF-2014M1A8A1049305). We are also indebted to the Spanish *Junta de Castilla y Leon* for its funding help (project VA248U13). Authors kindly acknowledge Sara Rodriguez by carrying out the gas separation tests. B.C-G is indebted to MINECO by a FPI scholarship.

Supporting Information

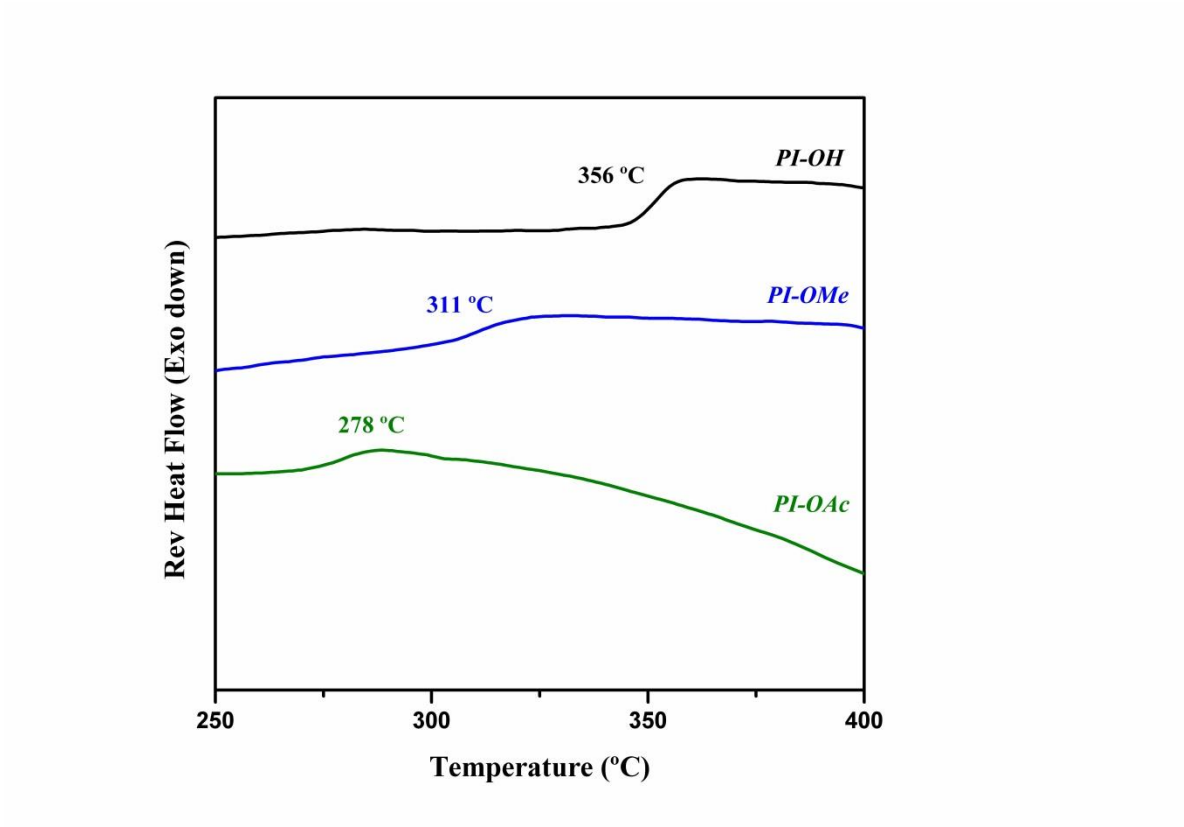

Fig.S1. Glass transition temperatures of precursor polyimides determined by MTDSC.

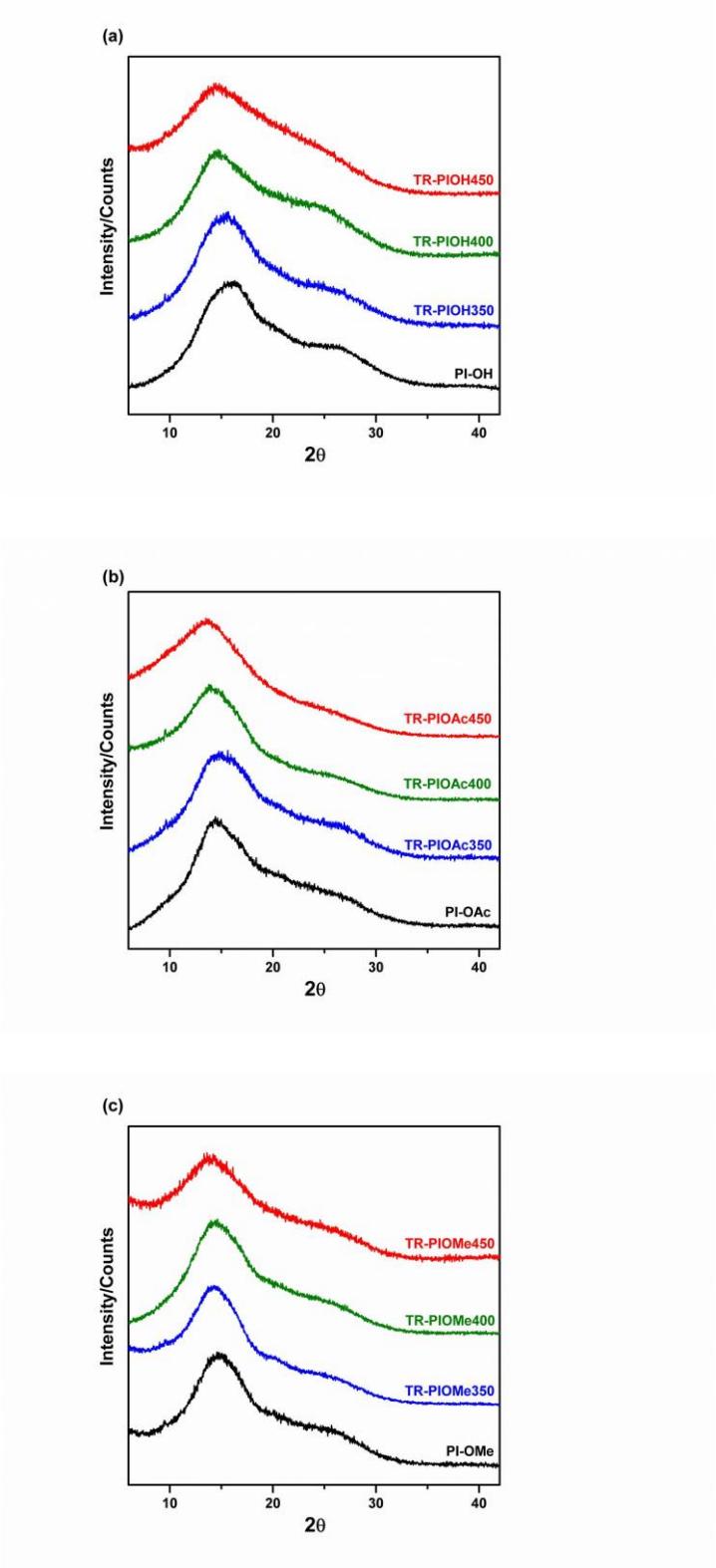

Fig. S2. Wide angle X-ray diffraction (WAXD) patterns of (a) PI-OH, (b) PI-OAc and (c) PI-OMe precursor polyimides along with the TR derived membranes, treated at different temperatures and heating times.

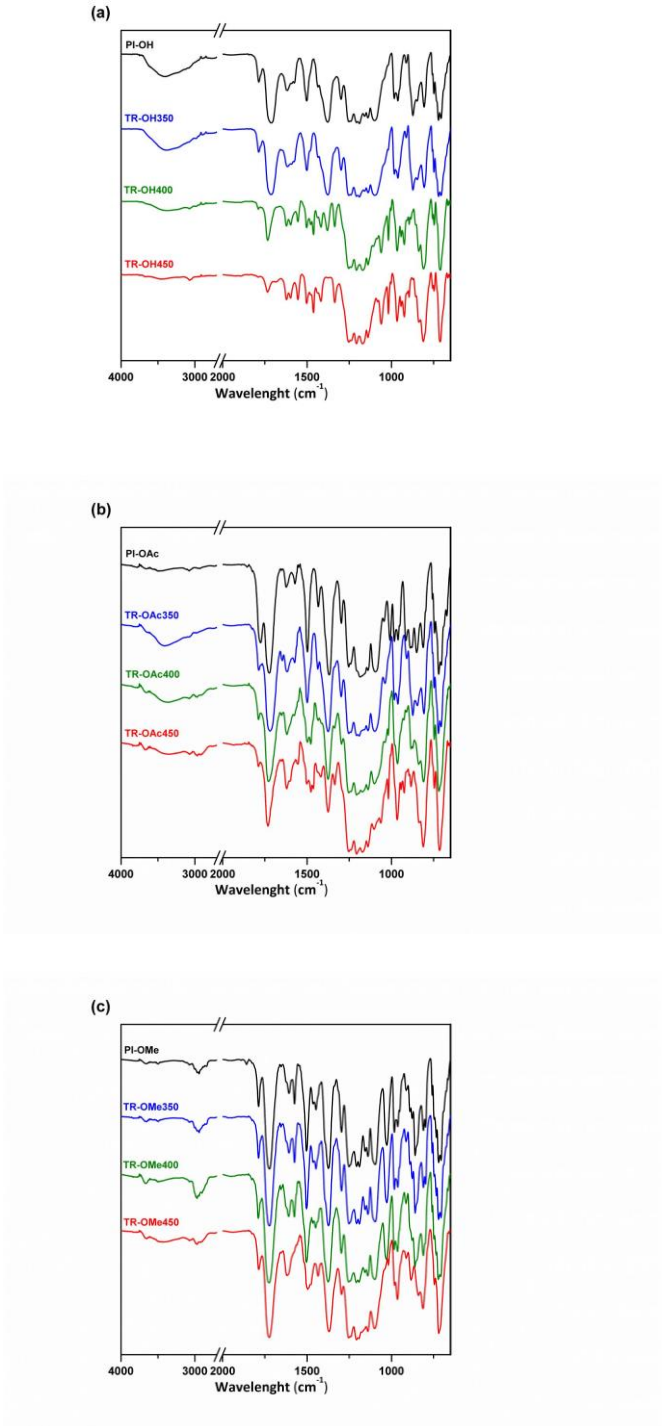

Fig. S3. ATR-FTIR spectra of (a) *PI-OH*, (b) *PI-OAc* and (c) *PI-OMe* precursor polyimides and thermally rearranged analog membranes, treated at different temperatures and heating times.

[1] K. Ghosal, B. Freeman, Gas separation using polymer membranes: An overview, Polym. Adv. Technol. 5 (1994) 673–697.

[2] W.J. Koros, G.K. Fleming, Membrane-based gas separation, J. Memb. Sci. 83 (1993) 1–80.

[3] P. Bernardo, E. Drioli, G. Golemme, Membrane gas separation: A review/state of the art, Ind. Eng. Chem. Res. 48 (2009) 4638–4663.

[4] Y. Yampolskii, B. Freeman, Membrane Gas Separation, John Wiley and Sons, 2010.

[5] J.K. Adewole, A.L. Ahmad, S. Ismail, C.P. Leo, Current challenges in membrane separation of CO2 from natural gas: A review, Int. J. Greenh. Gas Control. 17 (2013) 46–65.

[6] B.C. Bhide, S.A. Stern, A new evaluation of membrane processes for the oxygen-enrichment of air. I. Identification of optimum operating conditions and process configuration, J. Memb. Sci. 62 (1991) 13–35.

[7] A.A. Belyaev, Y.P. Yampolskii, L.E. Starannikova, A.M. Polyakov, G. Clarizia, E. Drioli, et al., Membrane air separation for intensification of coal gasification process, Fuel Process. Technol. 80 (2003) 119–141.

[8] S. Mokhatab, W.A. Poe, Chapter 7 - Natural Gas Sweetening, in: Handb. Nat. Gas Transm. Process. (Second Ed., 2012: pp. 253–290. doi:10.1016/B978-0-12-386914-2.00007-8.

[9] B.D. Bhide, S.A. Stern, Membrane processes for the removal of acid gases from natural gas. I. Process configurations and optimization of operating conditions, J. Memb. Sci. 81 (1993) 209–237.

[10] S. Sircar, T.C. Golden, M.B. Rao, Activated carbon for gas separation and storage, Carbon N. Y. 34 (1996) 1–12.

[11] V. V. Usachov, V. V. Teplyakov, A.Y. Okunev, N.I. Laguntsov, Membrane contactor air conditioning system: Experience and prospects, Sep. Purif. Technol. 57 (2007) 502–506.

[12] J.W. Phair, S.P.S. Badwal, Materials for separation membranes in hydrogen and oxygen production and future power generation, Sci. Technol. Adv. Mater. 7 (2006) 792–805. doi:10.1016/j.stam.2006.11.005.

[13] D.E. Jiang, V.R. Cooper, S. Dai, Porous graphene as the ultimate membrane for gas separation, Nano Lett. 9 (2009) 4019–4024.

[14] R.J. Lahiere, M.W. Hellums, Recovery of vinyl chloride monomer from PVC reactor vents, Membr. Technol. 1993 (1993) 5. doi:10.1016/0958-2118(93)90010-J.

[15] M. Askari, T.-S. Chung, Natural gas purification and olefin/paraffin separation using thermal cross-linkable co-polyimide/ZIF-8 mixed matrix membranes, J. Memb. Sci. 444 (2013) 173–183. doi:10.1016/j.memsci.2013.05.016.

[16] M. Das, W.J. Koros, Performance of 6FDA-6FpDA polyimide for propylene/propane separations, J. Memb. Sci. 365 (2010) 399–408. doi:10.1016/j.memsci.2010.09.029.

[17] C. Staudt-Bickel, W.J. Koros, Olefin/paraffin gas separations with 6FDA-based polyimide membranes, J. Memb. Sci. 170 (2000) 205–214. doi:10.1016/S0376-7388(99)00351-8.

[18] H. Herzog, An Introduction to CO2 Separation and Capture Technologies, Most. (1999) 1–8.

[19] X. Zhang, X. He, T. Gundersen, Post-combustion carbon capture with a gas separation membrane: Parametric study, capture cost, and exergy analysis, in: Energy and Fuels, 2013: pp. 4137–4149.

[20] L.M. Robeson, Correlation of separation factor versus permeability for polymeric membranes, J. Memb. Sci. 62 (1991) 165–185. doi:http://dx.doi.org/10.1016/0376-7388(91)80060-J.

[21] B.D. Freeman, Basis of Permeability/Selectivity Tradeoff Relations in Polymeric Gas Separation Membranes, Macromolecules. 32 (1999) 375–380.

[22] C.H. Lau, P. Li, F. Li, T.S. Chung, D.R. Paul, Reverse-selective polymeric membranes for gas separations, Prog. Polym. Sci. 38 (2013) 740–766. doi:10.1016/j.progpolymsci.2012.09.006.

[23] H.B. Park, C.H. Jung, Y.M. Lee, A.J. Hill, S.J. Pas, S.T. Mudie, et al., Polymers with cavities tuned for fast selective transport of small molecules and ions., Science. 318 (2007) 254–8. doi:10.1126/science.1146744.

[24] G.L. Tullos, J.M. Powers, S.J. Jeskey, L.J. Mathias, Thermal Conversion of Hydroxy-Containing Imides to Benzoxazoles: Polymer and Model Compound Study, Macromolecules. 32 (1999) 3598–3612. doi:10.1021/ma981579c.

[25] R. Guo, D.F. Sanders, Z.P. Smith, B.D. Freeman, D.R. Paul, J.E. McGrath, Synthesis and characterization of thermally rearranged (TR) polymers: effect of glass transition temperature of aromatic poly(hydroxyimide) precursors on TR process and gas permeation properties, J. Mater. Chem. A. 1 (2013) 262–272. doi:10.1039/c3ta10261k.

[26] J. Kostina, O. Rusakova, G. Bondarenko, A. Alentiev, T. Meleshko, N. Kukarkina, et al., Thermal rearrangement of functionalized polyimides: IR-

spectral, quantum chemical studies, and gas permeability of TR polymers, Ind. Eng. Chem. Res. 52 (2013) 10476–10483. doi:10.1021/ie3034043.

[27] E.-S. Yoo, A.J. Gavrin, R.J. Farris, E.B. Coughlin, Synthesis and Characterization of the Polyhydroxyamide/Polymethoxyamide Family of Polymers, High Perform. Polym. 15 (2003) 519–535. doi:10.1177/09540083030154008.

[28] S.I. Kim, T.J. Shin, S.M. Pyo, J.M. Moon, M. Ree, Structure and properties of rodlike poly(p-phenylene pyromellitimide)s containing short side groups, Polymer (Guildf). 40 (1999) 1603–1610. doi:10.1016/S0032-3861(98)00375-9.

[29] M. Al-Masri, D. Fritsch, H.R. Kricheldorf, New polyimides for gas separation. 2. Polyimides derived from substituted catechol bis(etherphthalic anhydride)s, Macromolecules. 33 (2000) 7127–7135. doi:10.1021/ma9920745.

[30] B. Comesaña-Gándara, M. Calle, H.J. Jo, A. Hernández, J.G. de la Campa, J. de Abajo, et al., Thermally rearranged polybenzoxazoles membranes with biphenyl moieties: Monomer isomeric effect, J. Memb. Sci. 450 (2014) 369–379. doi:10.1016/j.memsci.2013.09.010.

[31] M.J.S. Dewar, E.G. Zoebisch, E.F. Healy, J.J.P. Stewart, Development and use of quantum mechanical molecular models. 76. AM1: a new general purpose quantum mechanical molecular model, J. Am. Chem. Soc. 107 (1985) 3902–3909. doi:10.1021/ja00299a024.

[32] HyperChem(TM), Professional 8.0.3 Hypercube, Inc., Version 8.0.3, Florida, USA, (n.d.).

[33] D.M. Muñoz, M. Calle, J.G. de la Campa, J. de Abajo, A.E. Lozano, An Improved Method for Preparing Very High Molecular Weight Polyimides, Macromolecules. 42 (2009) 5892–5894. doi:10.1021/ma9005268.

[34] B. Comesaña-Gándara, A. Hernández, J.G. de la Campa, J. de Abajo, A.E. Lozano, Y. Moo Lee, Thermally rearranged polybenzoxazoles and poly(benzoxazole-co-imide)s from ortho-hydroxyamine monomers for high performance gas separation membranes, J. Memb. Sci. 493 (2015) 329–339. doi:10.1016/j.memsci.2015.05.061.

[35] M. Calle, Y.M. Lee, Thermally Rearranged (TR) Poly(ether−benzoxazole) Membranes for Gas Separation, Macromolecules. 44 (2011) 1156–1165. doi:10.1021/ma102878z.

[36] H.B. Park, S.H. Han, C.H. Jung, Y.M. Lee, A.J. Hill, Thermally rearranged (TR) polymer membranes for CO2 separation, J. Memb. Sci. 359 (2010) 11–24. doi:10.1016/j.memsci.2009.09.037.

[37] M. Pecullan, K. Brezinsky, I. Glassman, Pyrolysis and Oxidation of Anisole near 1000 K, J. Phys. Chem. A. 101 (1997) 3305–3316. doi:10.1021/jp963203b.

[38] G. Tullos, L. Mathias, Unexpected thermal conversion of hydroxy-containing polyimides to polybenzoxazoles, Polymer (Guildf). 40 (1999) 3463–3468. doi:10.1016/S0032-3861(98)00555-2.

[39] M. Calle, Y. Chan, H.J. Jo, Y.M. Lee, The relationship between the chemical structure and thermal conversion temperatures of thermally rearranged (TR) polymers, Polymer (Guildf). 53 (2012) 2783–2791. doi:10.1016/j.polymer.2012.04.032.

[40] D. Guzmán-Lucero, D. Likhatchev, Imide-to-benzoxazole rearrangement in ortho substituted poly(4-4′-diphenylene pyromellitimide)s, Polym. Bull. 48 (2002) 261–269. doi:10.1007/s00289-002-0038-7.

[41] J.H. Hodgkin, M.S. Liu, B.N. Dao, J. Mardel, A.J. Hill, Reaction mechanism and products of the thermal conversion of hydroxy-containing polyimides, Eur. Polym. J. 47 (2011) 394–400. doi:10.1016/j.eurpolymj.2010.12.014.

[42] J.H. Hodgkin, B.N. Dao, Thermal conversion of hydroxy-containing polyimides to polybenzoxazoles. Does this reaction really occur?, Eur. Polym. J. 45 (2009) 3081–3092. doi:10.1016/j.eurpolymj.2009.08.014.

[43] C. a. Scholes, C.P. Ribeiro, S.E. Kentish, B.D. Freeman, Thermal rearranged poly(benzoxazole-co-imide) membranes for CO2 separation, J. Memb. Sci. 450 (2014) 72–80. doi:10.1016/j.memsci.2013.08.049.

[44] Z.P. Smith, D.F. Sanders, C.P. Ribeiro, R. Guo, B.D. Freeman, D.R. Paul, et al., Gas sorption and characterization of thermally rearranged polyimides based on 3,3’-dihydroxy-4,4'-diamino-biphenyl (HAB) and 2,2'-bis-(3,4-dicarboxyphenyl) hexafluoropropane dianhydride (6FDA), J. Memb. Sci. 415-416 (2012) 558–567. doi:10.1016/j.memsci.2012.05.050.

[45] M. Calle, A.E. Lozano, Y.M. Lee, Formation of thermally rearranged (TR) polybenzoxazoles: Effect of synthesis routes and polymer form, Eur. Polym. J. 48 (2012) 1313–1322. doi:10.1016/j.eurpolymj.2012.04.007.

[46] O.Y. Rusakova, Y. V. Kostina, a. S. Rodionov, G.N. Bondarenko, a. Y. Alent’ev, T.K. Meleshko, et al., Study of the mechanism of the thermochemical reaction of polyimides with hydroxyl groups via vibrational-spectroscopy and quantum-chemistry methods, Polym. Sci. Ser. A. 53 (2011) 791–799. doi:10.1134/S0965545X11080074.

[47] S. Li, H.J. Jo, S.H. Han, C.H. Park, S. Kim, P.M. Budd, et al., Mechanically robust thermally rearranged (TR) polymer membranes with spirobisindane for gas separation, J. Memb. Sci. 434 (2013) 137–147. doi:10.1016/j.memsci.2013.01.011.